Journal of Scientific Computing (2024) 98:35
https://doi.org/10.1007/s10915-023-02418-9

Recovery Type a Posteriori Error Estimation of an Adaptive Finite Element Method for Cahn–Hilliard Equation

Yaoyao Chen[1] · Yunqing Huang[2] · Nianyu Yi[3] · Peimeng Yin[4]

Received: 7 May 2023 / Revised: 17 October 2023 / Accepted: 16 November 2023

Abstract
In this paper, we derive a novel recovery type a posteriori error estimation of the Crank–Nicolson finite element method for the Cahn–Hilliard equation. To achieve this, we employ both the elliptic reconstruction technique and a time reconstruction technique based on three time-level approximations, resulting in an optimal a posteriori error estimator. We propose a time-space adaptive algorithm that utilizes the derived a posteriori error estimator as error indicators. Numerical experiments are presented to validate the theoretical findings, including comparing with an adaptive finite element method based on a residual type a posteriori error estimator.

Keywords Cahn–Hilliard equation · A posteriori error estimation · Recovery type · Time-space adaptive algorithm

Mathematics Subject Classification 65N15 · 65N30 · 65N50

✉ Peimeng Yin
pyin@utep.edu

Yaoyao Chen
cyy1012xtu@126.com

Yunqing Huang
huangyq@xtu.edu.cn

Nianyu Yi
yinianyu@xtu.edu.cn

1 School of Mathematics and Statistics, Anhui Normal University, Wuhu 241000, People's Republic of China

2 Key Laboratory of Intelligent Computing and Information Processing of Ministry of Education, School of Mathematics and Computational Science, Xiangtan University, Xiangtan 411105, Hunan, People's Republic of China

3 Hunan Key Laboratory for Computation and Simulation in Science and Engineering, School of Mathematics and Computational Science, Xiangtan University, Xiangtan 411105, Hunan, People's Republic of China

4 Department of Mathematical Sciences, The University of Texas at El Paso, El Paso, TX 79968, USA

1 Introduction

In this paper, we are interested in an adaptive finite element method for the Cahn–Hilliard equation

$$\begin{cases} u_t + \mathcal{A}\left(\varepsilon \mathcal{A} u + \frac{1}{\varepsilon} f(u)\right) = 0, & \text{in } \Omega \times (0, T], \\ \partial_{\mathbf{n}} u \mid_{\partial\Omega} = 0, & \text{on } \partial\Omega \times [0, T], \\ \partial_{\mathbf{n}} \left(\varepsilon \mathcal{A} u + \frac{1}{\varepsilon} f(u)\right) \mid_{\partial\Omega} = 0, & \text{on } \partial\Omega \times [0, T], \\ u(x, 0) = u_0, & \text{in } \Omega \times \{t = 0\}, \end{cases} \tag{1.1}$$

where $\Omega \subset R^d (d = 2, 3)$ is a bounded domain with Lipschitz boundary $\partial\Omega$, $\mathbf{n}$ is the unit outward normal to the boundary $\partial\Omega$, and the small parameter $\varepsilon > 0$ represents thickness of the interface layer, and the operator $\mathcal{A} := -\Delta$. The nonlinear function $f(u) = F^{'}(u) = u^3 - u$ with $F(u) = \frac{1}{4}(u^2 - 1)^2$, which is a double well potential and drives the solution to two pure states $u = \pm 1$.

The Cahn–Hilliard equation, which was introduced by Cahn and Hilliard in the late 1950s to describe the process of phase separation [8], has become a fundamental model in engineering and materials science. It also plays an increasingly important role in many other fields [6, 16]. The Cahn–Hilliard equation can be expressed as the H^{-1}-gradient flow, given by $u_t = \nabla \cdot (\delta_u E(u))$, where $\delta_u E(u)$ is the variational derivative of the total free energy functional

$$E(u) = \int_\Omega \left(\frac{\varepsilon}{2} |\nabla u|^2 + \frac{1}{\varepsilon} F(u)\right) dx.$$

It is well-known that the Cahn–Hilliard equation (1.1), subject to the prescribed boundary conditions, satisfies an energy dissipative law given by

$$\frac{d}{dt} E(u(t)) = -(u_t, u_t) \le 0.$$

Efficient and easy-to-implement numerical methods for the Cahn–Hilliard equation face several challenges, including the presence of high order derivatives, a nonlinear reaction term $f(u)$, and the smallness of the parameter ε. To overcome these challenges, many spatial discretizations have been studied, including finite difference methods [12], finite element methods [14, 20, 32], discontinuous Galerkin methods [18, 19, 37, 43], and spectral methods [15]. Strategies to address the nonlinearity include convex-splitting methods [25], stabilization methods [42], invariant energy quantization (IEQ) approach [37, 45], and scalar variable auxiliary (SAV) approach [28, 40, 41]. Numerical approximations of the Cahn–Hilliard equation have been extensively investigated, but efficient and accurate methods are still an active area of research.

The smallness of the parameter ε in gradient flow models, including the Cahn–Hilliard equation and the Allen–Cahn equation, results in the interface layer phenomenon. To accurately simulate macroscopic processes described by these equations, it is necessary to use adaptive techniques to adjust the spatial mesh size and time step size according to the interface width ε. In recent years, some works on a posteriori error estimators and adaptive methods have been proposed. Feng and Wu [21] developed residual-type a posteriori error estimates for conforming and mixed finite element approximations of the Cahn–Hilliard equation. A superconvergent cluster recovery (SCR)-based a posteriori error estimation and a time-space adaptive finite element algorithm was proposed in [10] for the Allen–Cahn equation. The SCR method produces a superconvergent recovered gradient, which leads to an asymptotically exact SCR-based error estimator. The primary focus of [10] was to design an adaptive algorithm based on the SCR-based error estimator, while the time adaptation of the error indicator was simply constructed based on approximations on two time levels.

In this paper, we present a novel SCR-based recovery type a posteriori error estimator for the Crank–Nicolson finite element method applied to the Cahn–Hilliard equation. The a posterior error estimator is derived using both the elliptic reconstruction technique and the time reconstruction technique, and similar techniques have been employed to study the Allen–Cahn equation [13, 22]. Therefore, the a posterior error estimator constructed is of greater precision and efficiency. The elliptic reconstruction technique, introduced in [33, 39] for parabolic problems, involves separating the error between the finite element approximation and the exact solution into two categories: elliptic type and parabolic type. The key idea is to leverage pre-existing elliptic a posteriori estimators for the elliptic type error, while controlling the parabolic type error using parabolic energy estimates. In [11], a time reconstruction technique using approximations on two time levels was introduced for the Allen–Cahn equation, which allowed for the construction of a first-order a posteriori error estimator for time discretization. In this work, we utilize the time reconstruction technique involving approximations on three time levels [38], leading to a second-order a posteriori error estimator for time discretization. We employ the derived a posteriori error estimator as error indicators and propose an efficient time-space adaptive algorithm to solve the Cahn–Hilliard equation. Our numerical results show that the proposed recovery type a posteriori error estimator is more effective than a residual type error estimator and a space-only adaptive algorithm. Furthermore, our results demonstrate that the use of time step adaptation is essential in achieving accurate numerical solutions for the Cahn–Hilliard equation.

The paper is organized as follows: In Sect. 2, we introduce the Crank–Nicolson finite element method for discretizing the Cahn–Hilliard equation, followed by an introduction of the elliptic reconstruction for a nonlinear elliptic problem and its properties. In Sect. 3, we derive an optimal a posteriori error estimation for the Cahn–Hilliard equation based on the elliptic reconstruction and time reconstruction techniques. Based on the derived error estimator, we propose a time-space adaptive algorithm. In Sect. 4, we present several numerical examples to verify the accuracy and effectiveness of the proposed error indicators and the corresponding time-space adaptive algorithm. We present concluding remarks in Sect. 5. Finally, in "Appendix A", we provide the proof of Theorem 3.2.

2 The Discrete Scheme and Elliptic Reconstruction

For a bounded domain $\Omega \subset R^d$, we adopt the standard notations for the Sobolev space $W^{m,p}(\Omega)$ equipped with the norm $\|\cdot\|_{m,p,\Omega}$ and the semi-norm $|\cdot|_{m,p,\Omega}$. If $p = 2$, we set $W^{m,p}(\Omega) = H^m(\Omega)$, $\|\cdot\|_{m,p,\Omega} = \|\cdot\|_{m,\Omega}$ and $|\cdot|_{m,p,\Omega} = |\cdot|_{m,\Omega}$. Further, if $m = 2$, we take $\|\cdot\| = \|\cdot\|_{0,\Omega}$. We also denote by $L^p(0, T; H^k(\Omega))$ the space of all L^p integrable functions from $(0, T)$ into $H^k(\Omega)$ with norm $\|v\|_{L^p(0,T;H^k(\Omega))} = \left(\int_0^T \|v\|_{k,\Omega}^p dt\right)^{\frac{1}{p}}$ for $p \in [1, \infty)$. Similarly, one can define the space $H^1(0, T; H^k(\Omega))$. Especially, we denote $V = L^2(0, T; H^1(\Omega))$.

By introducing the chemical potential

$$w := \varepsilon \mathcal{A} u + \frac{1}{\varepsilon} f(u), \tag{2.1}$$

(1.1) can be equivalently written as

$$\begin{cases} u_t + \mathcal{A} w = 0, & \text{in } \Omega \times (0, T], \\ \partial_{\mathbf{n}} w \mid_{\partial\Omega} = 0, & \text{on } \partial\Omega \times [0, T], \\ \varepsilon \mathcal{A} u + \frac{1}{\varepsilon} f(u) - w = 0, & \text{in } \Omega \times (0, T], \\ \partial_{\mathbf{n}} u \mid_{\partial\Omega} = 0, & \text{on } \partial\Omega \times [0, T], \\ u(x, 0) = u_0, & \text{in } \Omega \times \{t = 0\}. \end{cases} \tag{2.2}$$

Given initial data $u_0 \in H^2(\Omega)$, problem (2.2) admits a unique global solution (u, w), we refer to [17] and references therein for more discussions on well-posedness and regularity.

2.1 The Crank–Nicolson Finite Element Scheme

For the homogeneous Neumann boundary conditions, the problem (2.2) is understood in the following weak form: find $(u, w) \in \left(H^1(0, T; L^2(\Omega)) \cap V\right) \times V$ such that

$$\begin{cases} (u_t, v) + a(w, v) = 0, & \forall v \in H^1(\Omega), \\ \varepsilon a(u, \varphi) + \frac{1}{\varepsilon}\big(f(u), \varphi\big) - (w, \varphi) = 0, & \forall \varphi \in H^1(\Omega), \\ u(\cdot, 0) = u_0, & \end{cases} \tag{2.3}$$

here $a(\cdot, \cdot)$ is a bilinear form on $H^1(\Omega)$ defined by

$$a(v, \varphi) := (\nabla v, \nabla \varphi), \qquad \forall v, \varphi \in H^1(\Omega).$$

Existence and uniqueness of weak solutions with initial data $u_0 \in H^2(\Omega)$ was proved in [17, 20].

Let $\mathcal{T}_h$ be a shape regular triangulation of Ω, and V_h be the corresponding finite element space, which is defined as

$$V_h := \left\{v \in H^1(\Omega), v|_K \in P_1(K), \forall\, K \in \mathcal{T}_h\right\},$$

where $P_1(K)$ denotes the set of linear polynomials defined in K. The semi-discrete finite element scheme of (2.2) reads: find $(u_h, w_h) \in H^1(0, T; V_h) \times L^2(0, T; V_h)$ such that

$$\begin{cases} (u_{h,t}, v_h) + a(w_h, v_h) = 0, & \forall v_h \in V_h, \\ \varepsilon a(u_h, \varphi_h) + \frac{1}{\varepsilon}\big(f(u_h), \varphi_h\big) - (w_h, \varphi_h) = 0, & \forall \varphi_h \in V_h, \\ (u_h(x, 0) - u_0, \phi_h) = 0, & \forall \phi_h \in V_h. \end{cases} \tag{2.4}$$

Generally, we rewrite the scheme (2.4) in its pointwise form

$$\begin{cases} u_{h,t} + A w_h = 0, \\ \varepsilon A u_h + \frac{1}{\varepsilon} P f(u_h) - w_h = 0, \\ u_h(x, 0) = u_h^0 := P u_0, \end{cases} \tag{2.5}$$

where the finite-dimensional space operator $A : V_h \to V_h$ is the discrete Laplacian defined, through the Riesz representation in V_h, by

$$\langle A v_h, \Phi\rangle = a(v_h, \Phi), \qquad \forall \Phi \in V_h, \tag{2.6}$$

and $P : L^2(\Omega) \to V_h$ is the $L^2(\Omega)$-projection operator such that, for each $\upsilon \in L^2(\Omega)$, we have

$$(P\upsilon, \Phi) = \langle \upsilon, \Phi\rangle, \qquad \forall \Phi \in V_h. \tag{2.7}$$

We divide the time interval $[0, T]$ into a partition of N consecutive adjacent subintervals whose endpoints are denoted by $0 = t_0 < t_1 < \cdots < t_N = T$, the n-th time interval $I_n := [t_{n-1}, t_n]$ and the corresponding time step is defined as $\tau_n := t_n - t_{n-1}$. The Crank–Nicolson finite element is to find a sequence of functions $(u_h^n, w_h^n) \in V_h \times V_h$ such that, for each $n = 1, 2, \ldots, N$,

$$\begin{cases} \left(\dfrac{u_h^n - u_h^{n-1}}{\tau_n}, v_h\right) + \dfrac{1}{2} a\left(w_h^n + w_h^{n-1}, v_h\right) = 0, \qquad \forall v_h \in V_h, \\ \dfrac{\varepsilon}{2} a\left(u_h^n + u_h^{n-1}, \varphi_h\right) + \dfrac{1}{\varepsilon}\left(\dfrac{f(u_h^n) + f(u_h^{n-1})}{2}, \varphi_h\right) \\ \qquad -\dfrac{1}{2}\left(w_h^n + w_h^{n-1}, \varphi_h\right) = 0, \qquad \forall \varphi_h \in V_h, \\ u_h(x, 0) = u_h^0. \end{cases} \tag{2.8}$$

Similarly to the semi-discrete scheme, the fully discrete scheme can be written in a pointwise form as follows

$$\begin{cases} \dfrac{u_h^n - u_h^{n-1}}{\tau_n} + \dfrac{1}{2}\left(A w_h^n + A w_h^{n-1}\right) = 0, \\ \dfrac{\varepsilon}{2}\left(A u_h^n + A u_h^{n-1}\right) + \dfrac{P f(u_h^n) + P f(u_h^{n-1})}{2\varepsilon} - \dfrac{1}{2}\left(w_h^n + w_h^{n-1}\right) = 0, \\ u_h(x, 0) = u_h^0. \end{cases} \tag{2.9}$$

2.2 Elliptic Reconstruction

The nonlinear elliptic problem corresponding to a steady state of the nonlinear evolution equation (1.1) is taken as follows: given $g \in L^2(\Omega)$, $r \in L^2(\Omega)$, find $(\mu, \nu) \in H^1(\Omega) \times H^1(\Omega)$ such that

$$\begin{cases} \mathcal{A}\nu + \nu = g, \qquad \text{in } \Omega, & (2.10a) \\ \varepsilon\mathcal{A}\mu + \dfrac{1}{\varepsilon} h(\mu) - \nu = r, \qquad \text{in } \Omega, & (2.10b) \\ \nabla\mu \cdot \mathbf{n} = 0,\ \nabla\nu \cdot \mathbf{n} = 0, \qquad \text{on } \partial\Omega, & (2.10c) \end{cases}$$

with $h(\mu) := \mu^3$. The weak form of the elliptic problem (2.10a)–(2.10c) reads: find $(\mu, \nu) \in H^1(\Omega) \times H^1(\Omega)$ such that

$$a(\nu, v) + (\nu, v) = \langle g, v\rangle, \qquad \forall v \in H^1(\Omega), \tag{2.11}$$

$$\varepsilon a(\mu, \varphi) + \frac{1}{\varepsilon}(h(\mu), \varphi) - (\nu, \varphi) = \langle r, \varphi\rangle, \qquad \forall \varphi \in H^1(\Omega). \tag{2.12}$$

Remark 2.1 The well-posedness of the variational problem (2.11)–(2.12) can be derived as follows. Note that the variational problem (2.11) is the Euler-Lagrange equation of the functional

$$J(\nu) = \frac{1}{2}\int_\Omega |\nabla \nu|^2 + \frac{1}{2}\int_\Omega \nu^2 - \int_\Omega g\nu. \tag{2.13}$$

By taking the derivative of the functional $J(\nu)$, it holds that

$$\left(\frac{\delta J(\nu)}{\delta \nu}, v\right) = a(\nu, v) + (\nu, v) - (g, v) = 0, \quad \forall v \in H^1(\Omega). \tag{2.14}$$

Notice that $J(\nu)$ is a convex functional, then the uniqueness of the solution for scheme (2.11) is proved. As for the variational problem (2.12), it is the Euler-Lagrange equation of the functional

$$H(\mu) = \frac{\varepsilon}{2}\int_\Omega |\nabla \mu|^2 + \frac{1}{4\varepsilon}\int_\Omega \mu^4 - \int_\Omega s\mu, \tag{2.15}$$

where $\int_\Omega s\mu := (\nu, \mu) + \langle r, \mu\rangle$. Similarly, taking the derivative of the functional $H(\mu)$, it has

$$\left(\frac{\delta H(\mu)}{\delta \mu}, \varphi\right) = \varepsilon a(\mu, \varphi) + \frac{1}{\varepsilon}(h(\mu), \varphi) - (s, \varphi) = 0, \quad \forall \varphi \in H^1(\Omega). \tag{2.16}$$

Since $H(\mu)$ is a convex functional, it yields the uniqueness of the solution for scheme (2.12).

The finite element discretization of the elliptic problem (2.10a)–(2.10c) reads: find $(\mu_h, \nu_h) \in V_h \times V_h$ such that

$$\begin{cases} a(\nu_h, v_h) + (\nu_h, v_h) = \langle g_h, v_h\rangle, & \forall v_h \in V_h, \\ \varepsilon a(\mu_h, \varphi_h) + \frac{1}{\varepsilon}(h(\mu_h), \varphi_h) - (\nu_h, \varphi_h) = \langle r_h, \varphi_h\rangle, & \forall \varphi_h \in V_h. \end{cases} \tag{2.17}$$

Definition 2.1 (*Gradient recovery a posteriori estimator function*) For the nonlinear elliptic problem (2.10a)–(2.10c), we define the gradient recovery a posteriori estimator functional

$$\mathcal{E}_v := \mathcal{E}[v_h, H^1(\Omega), V_h] := \|Gv_h - \nabla v_h\|, \qquad \forall v_h \in V_h, \tag{2.18}$$

where G is a gradient recovery operator.

Remark 2.2 As in [34], we utilize $H^1(\Omega)$ to estimate the elliptic a posteriori estimation for the gradient recovery a posteriori estimator functional $\mathcal{E}_v$. However, it's worth noting that there are alternative methods to compute upper and lower bounds for the error in other functional spaces, such as $L^2(\Omega)$ and $L^\infty(\Omega)$.

Gradient recovery is a post-processing technique that has gained widespread popularity in the engineering community for its robustness as an a posteriori error estimator, its superconvergence of the recovered derivatives, and its efficiency in implementation. It involves reconstructing gradient approximations from finite element solutions to obtain improved solutions. The practical use of the recovery technique is not only to enhance the quality of the approximation but also to construct a posteriori error estimators in adaptive computation. The gradient of the finite element approximation for the Lagrange element provides a discontinuous approximation to the true gradient. Various techniques have been proposed to recover the gradient, including averaging [7, 29], local or global projections [27, 30], postprocessing interpolation [36, 44], the superconvergent patch recovery (SPR) [47], the polynomial preserving recovery (PPR) [48] and the superconvergent cluster recovery (SCR) [31].

Assumption 2.1 (*Elliptic a posteriori error estimators*) [34] Assume that (μ, ν), (μ_h, ν_h) are the exact solution and numerical solution of nonlinear elliptic problem (2.10a)–(2.10c), respectively, $\mathcal{E}$ defined as Definition 2.1, there exists constants C_0 and C_1, such that the following bounds hold

$$\begin{aligned} \|\nabla(\mu_h - \mu)\| &\leq C_0 \mathcal{E}_\mu, \\ \|\nabla(\nu_h - \nu)\| &\leq C_1 \mathcal{E}_\nu. \end{aligned} \tag{2.19}$$

Remark 2.3 The basic idea of the gradient recovery based a posteriori error estimator is to reconstruct a "better" gradient approximation by the so-called recovery technique. If the recovered gradient is more accurate than the gradient of the finite element approximation, that is

$$\|G\vartheta_h - \nabla\vartheta\| \leq \beta \|\nabla\vartheta - \nabla\vartheta_h\|, \quad 0 \leq \beta < 1, \tag{2.20}$$

where $\vartheta = \mu, \ \nu$, and ϑ_h denotes the numerical solution of ϑ. Applying the triangle inequalities to (2.20), we can derive the efficiency and reliability of the error estimator

$$\frac{1}{1+\beta}\|G\vartheta_h - \nabla\vartheta_h\| \leq \|\nabla\vartheta - \nabla\vartheta_h\| \leq \frac{1}{1-\beta}\|G\vartheta_h - \nabla\vartheta_h\|.$$

Furthermore, if the recovery gradient has the superconvergence property

$$\|G\vartheta_h - \nabla\vartheta\| = o(\|\nabla\vartheta - \nabla\vartheta_h\|), \qquad (\beta \to 0 \text{ as } h \to 0)$$

then the corresponding recovery type a posteriori error estimator $\|G\vartheta_h - \nabla\vartheta_h\|$ is an asymptotic approximation to $\|\nabla\vartheta - \nabla\vartheta_h\|$, that is

$$\frac{\|G\vartheta_h - \nabla\vartheta_h\|}{\|\nabla\vartheta - \nabla\vartheta_h\|} \to 1, \qquad \text{as } h \to 0.$$

In addition, the recovery type error estimator is usually problem independent. Therefore, the constants C_0 and C_1 in Assumption 2.1 are independent of the parameters in the model (2.10b).

To link the Cahn–Hilliard equation and the elliptic recovered gradient estimates, we utilize the elliptic reconstruction technique.

Definition 2.2 (*Elliptic reconstruction*) For $1 \leq n \leq N$ with the discrete elliptic operator A defined as (2.6), we define the corresponding elliptic reconstruction operator $R : V_h \to H^1(\Omega)$, for each $(\chi, \vartheta) \in V_h \times V_h$, by solving for the elliptic problem

$$\begin{cases} \mathcal{A}R\vartheta + R\vartheta = A\vartheta + \vartheta, \\ \varepsilon\mathcal{A}R\chi + \dfrac{1}{\varepsilon}h(R\chi) - R\vartheta = \varepsilon A\chi + \dfrac{1}{\varepsilon}Ph(\chi) - \vartheta, \end{cases} \tag{2.21}$$

which can be written in weak form as

$$\begin{cases} a(R\vartheta, v) + (R\vartheta, v) = \langle A\vartheta, v\rangle + (\vartheta, v), \ \forall v \in H^1(\Omega), \\ \varepsilon a(R\chi, \varphi) + \dfrac{1}{\varepsilon}(h(R\chi), \varphi) - (R\vartheta, \varphi) = \varepsilon\langle A\chi, \varphi\rangle + \dfrac{1}{\varepsilon}\langle h(\chi), \varphi\rangle - \langle\vartheta, \varphi\rangle, \ \forall\varphi \in H^1(\Omega). \end{cases} \tag{2.22}$$

By the Definition 2.2, it is obviously that (Ru_h^n, Rw_h^n), (u_h^n, w_h^n) are the exact solution and numerical solution of (2.21), respectively. According to Assumption 2.1, we have

$$\|\nabla(u_h^n - Ru_h^n)\| \leq C_0\mathcal{E}_u^n, \tag{2.23}$$

$$\|\nabla(w_h^n - Rw_h^n)\| \leq C_1\mathcal{E}_w^n, \tag{2.24}$$

where $\mathcal{E}_u^n,\ \mathcal{E}_w^n$ are defined following Definition 2.1, respectively, by

$$\mathcal{E}_u^n := \|Gu_h^n - \nabla u_h^n\|, \qquad \forall u_h^n \in V_h, \tag{2.25}$$

$$\mathcal{E}_w^n := \|Gw_h^n - \nabla w_h^n\|, \qquad \forall w_h^n \in V_h. \tag{2.26}$$

3 A Posteriori Error Estimation and Adaptive Algorithm

In this section, we derive a recovery type a posteriori error estimation for the Cahn–Hilliard equation based on the elliptic reconstruction and time reconstruction techniques, and a time-space adaptive algorithm is also developed based on the proposed a posteriori error estimation.

3.1 A Posteriori Error Estimation

The discrete solution is sequence of finite element functions $u_h^n \in V_h^n$ defined at each discrete time t_n, $1 \leq n \leq N$. Define the piecewise quadratic extension [38]

$$\begin{aligned} u_h(t) &:= \frac{t - t_{n-1}}{\tau_n} u_h^n + \frac{t_n - t}{\tau_n} u_h^{n-1} + \frac{1}{2}(t - t_{n-1})(t - t_n)\partial_n^2 u_h,\ t \in I_n,\ 1 \leq n \leq N, \\ w_h(t) &:= \frac{t - t_{n-1}}{\tau_n} w_h^n + \frac{t_n - t}{\tau_n} w_h^{n-1} + \frac{1}{2}(t - t_{n-1})(t - t_n)\partial_n^2 w_h,\ t \in I_n,\ 1 \leq n \leq N, \end{aligned} \tag{3.1}$$

where the term $\partial_n^2 v_h$ is defined as

$$\partial_n^2 v_h := \frac{\frac{v_h^n - v_h^{n-1}}{\tau_n} - \frac{v_h^{n-1} - v_h^{n-2}}{\tau_{n-1}}}{\frac{\tau_n + \tau_{n-1}}{2}} \tag{3.2}$$

with $v_h^{-1} = v_h^0$ as $n = 1$.

Then we also define

$$p^n := Ru_h^n, \qquad q^n := Rw_h^n, \qquad n = 0, 1, 2, \ldots, N, \tag{3.3}$$

and denote this sequence's piecewise quadratic reconstruction in time by $p(t)$ and $q(t)$, that is,

$$\begin{aligned} p(t) &:= \frac{t - t_{n-1}}{\tau_n} p^n + \frac{t_n - t}{\tau_n} p^{n-1} + \frac{1}{2}(t - t_{n-1})(t - t_n)\partial_n^2 p, \quad t \in I_n,\ 1 \leq n \leq N, \\ q(t) &:= \frac{t - t_{n-1}}{\tau_n} q^n + \frac{t_n - t}{\tau_n} q^{n-1} + \frac{1}{2}(t - t_{n-1})(t - t_n)\partial_n^2 q, \quad t \in I_n,\ 1 \leq n \leq N. \end{aligned} \tag{3.4}$$

The corresponding fully discrete error is defined by

$$\begin{aligned} e_u &:= u_h(t) - u(t), \\ e_w &:= w_h(t) - w(t), \end{aligned} \tag{3.5}$$

and can be split, using the elliptic reconstruction $p(t)$ and $q(t)$, as follows

$$\begin{aligned} e_u &= (p(t) - u(t)) - (p(t) - u_h(t)) := \rho_u - \epsilon_u, \\ e_w &= (q(t) - w(t)) - (q(t) - w_h(t)) := \rho_w - \epsilon_w. \end{aligned} \tag{3.6}$$

For terms in (3.6), the following result holds.

Theorem 3.1 (Parabolic error identity) *For each $n = 1, 2, \ldots, N$ and each $t \in (t_{n-1}, t_n]$, it holds that*

$$\begin{aligned} \partial_t e_u + \mathcal{A}\rho_w &= \frac{Aw_h^n - Aw_h^{n-1}}{2} + \mathcal{A}(q(t) - q^n) + w_h^n - Rw_h^n + (t - t_{n-\frac{1}{2}})\partial_n^2 u_h, \\ \varepsilon\mathcal{A}\rho_u - \rho_w &= \varepsilon\frac{Au_h^n - Au_h^{n-1}}{2} + \frac{Pf(u_h^n) - Pf(u_h^{n-1})}{2\varepsilon} - \frac{w_h^n - w_h^{n-1}}{2} \\ &\quad + \varepsilon\mathcal{A}(p(t) - p^n) - (q(t) - q^n) + \frac{f(u) - f(p^n)}{\varepsilon} + \frac{1}{\varepsilon}\left(u_h^n - p^n\right). \end{aligned} \tag{3.7}$$

Proof For $n = 1, 2, \ldots, N$ and $t \in (t_{n-1}, t_n]$, by the definition of u_h^n, we have

$$\partial_t u_h = \frac{u_h^n - u_h^{n-1}}{\tau_n} + (t - t_{n-\frac{1}{2}})\partial_n^2 u_h,$$

and using the fully discrete scheme (2.9), we obtain

$$\begin{aligned} \partial_t u_h + \mathcal{A}q^n + q^n &= \frac{u_h^n - u_h^{n-1}}{\tau_n} + Aw_h^n + w_h^n + (t - t_{n-\frac{1}{2}})\partial_n^2 u_h \\ &= \frac{u_h^n - u_h^{n-1}}{\tau_n} + \frac{Aw_h^n + Aw_h^{n-1}}{2} + \frac{Aw_h^n - Aw_h^{n-1}}{2} \\ &\quad + w_h^n + (t - t_{n-\frac{1}{2}})\partial_n^2 u_h \\ &= \frac{Aw_h^n - Aw_h^{n-1}}{2} + w_h^n + (t - t_{n-\frac{1}{2}})\partial_n^2 u_h, \\ \varepsilon\mathcal{A}p^n + \frac{1}{\varepsilon}h(p^n) - q^n &= \varepsilon Au_h^n + \frac{1}{\varepsilon}Ph(u_h^n) - w_h^n \\ &= \varepsilon\frac{Au_h^n + Au_h^{n-1}}{2} + \varepsilon\frac{Au_h^n - Au_h^{n-1}}{2} + \frac{Ph(u_h^n) + Pf(u_h^{n-1})}{2\varepsilon} \\ &\quad + \frac{Ph(u_h^n) - Pf(u_h^{n-1})}{2\varepsilon} - \frac{w_h^n + w_h^{n-1}}{2} - \frac{w_h^n - w_h^{n-1}}{2} \\ &= \varepsilon\frac{Au_h^n - Au_h^{n-1}}{2} + \frac{Pf(u_h^n) - Pf(u_h^{n-1})}{2\varepsilon} - \frac{w_h^n - w_h^{n-1}}{2} \\ &\quad + \frac{1}{\varepsilon}u_h^n. \end{aligned}$$

Hence

$$\partial_t u_h + \mathcal{A}q(t) = \frac{Aw_h^n - Aw_h^{n-1}}{2} + \mathcal{A}(q(t) - q^n) + w_h^n - Rw_h^n + (t - t_{n-\frac{1}{2}})\partial_n^2 u_h,$$

$$\varepsilon \mathcal{A}p(t) + \frac{1}{\varepsilon}h(p^n) - q(t) = \varepsilon \frac{Au_h^n - Au_h^{n-1}}{2} + \frac{Pf(u_h^n) - Pf(u_h^{n-1})}{2\varepsilon} - \frac{w_h^n - w_h^{n-1}}{2} + \varepsilon \mathcal{A}(p(t) - p^n) - (q(t) - q^n) + \frac{1}{\varepsilon}u_h^n,$$

and subtracting (2.2) from the above formula, we get

$$\partial_t e_u + \mathcal{A}\rho_w = \frac{Aw_h^n - Aw_h^{n-1}}{2} + \mathcal{A}(q(t) - q^n) + w_h^n - Rw_h^n + (t - t_{n-\frac{1}{2}})\partial_n^2 u_h,$$

$$\varepsilon \mathcal{A}\rho_u - \rho_w = \varepsilon \frac{Au_h^n - Au_h^{n-1}}{2} + \frac{Pf(u_h^n) - Pf(u_h^{n-1})}{2\varepsilon} - \frac{w_h^n - w_h^{n-1}}{2} + \varepsilon \mathcal{A}(p(t) - p^n) - (q(t) - q^n) + \frac{f(u) - f(p^n)}{\varepsilon} + \frac{1}{\varepsilon}\left(u_h^n - p^n\right).$$

□

Then we have the following result.

Theorem 3.2 *Let $(u_h^n, w_h^n)_{n \in [0:N]}$ be the fully discrete solution, defined at each discrete time t_n, its piecewise linear extension $u_h,\ w_h$ defined as (3.1), and let $u,\ w$ be the exact solution of the model problem (2.2). Assume that $|u_h|_{L^\infty(0,T;L^\infty(\Omega))}$ is bounded independent of ε, and $\overline{\Lambda}_h \in L^1(0,T)$ for almost every $t \in (0,T)$ satisfies [2]*

$$-\overline{\Lambda}_h(t) \le -\Lambda_h(t) := \inf_{v \in \dot{V} \backslash \{0\}} \frac{\varepsilon \|\nabla v\|^2 + \varepsilon^{-1}(f'(u_h)v, v)}{\|\nabla \Delta^{-1} v\|^2}, \tag{3.8}$$

where $\overline{\Lambda}_h$ depends on the mesh size h. If we further assume

$$\eta^2 := \|\nabla \Delta^{-1} e_u^0\|^2 + \sum_{n=1}^{N} 4\varepsilon^{-2} \widetilde{\mathcal{E}}_u^{n\,2} + \sum_{n=1}^{N} \left(\eta_0^2 + \varepsilon^{-2}\eta_1^2\right)\tau_n$$

satisfies

$$\eta^2 \le \frac{\varepsilon^{1/\sigma}}{(2\mu_g C_S(1+T))^{1/\sigma}} \left(8 \exp\left(\int_0^T a(t)dt\right)\right)^{-1-\frac{1}{\sigma}},$$

for

$$a(t) := \left(6 + 2\left(1 - \varepsilon^3\right)\overline{\Lambda}_h(t)\right),$$

$$\mu_g := \sup_{t \in (0,T)} \|\tilde{f}(u_h)\|_{L^\infty(\Omega)},$$

with $\tilde{f}(u_h) = 3|u_h|$, then it holds

$$\sup_{t \in [0,T]} \|\nabla \Delta^{-1} e_u\|^2 + \int_0^T \frac{\varepsilon^4}{2}\|\nabla e_u\|^2 dt \le 8\eta^2 \exp\left(\int_0^T a(t)dt\right), \tag{3.9}$$

where

$$
\begin{aligned}
\widetilde{\mathcal{E}_u^n}^2 :=& \frac{C_0^2}{3}\tau_n\left((\mathcal{E}_u^n)^2 + (\mathcal{E}_u^{n-1})^2 + \mathcal{E}_u^n\mathcal{E}_u^{n-1}\right) \\
&+ C_0^2\frac{\tau_n^2\tau_{n-1}\left(\mathcal{E}_u^n + \mathcal{E}_u^{n-1}\right) + \tau_n^3\left(\mathcal{E}_{u-1}^n + \mathcal{E}_u^{n-2}\right)}{6\tau_{n-1}(\tau_n + \tau_{n-1})}\left(\mathcal{E}_u^n + \mathcal{E}_u^{n-1}\right) \\
&+ C_0^2\tau_n^3\frac{\left(\tau_{n-1}\left(\mathcal{E}_u^n + \mathcal{E}_u^{n-1}\right) + \tau_n\left(\mathcal{E}_{u-1}^n + \mathcal{E}_u^{n-2}\right)\right)^2}{30\tau_{n-1}^2(\tau_n + \tau_{n-1})^2}; \\
\eta_0 :=& \beta_u^n + \gamma_w^n + \delta_w^n + \eta_w^n; \\
\eta_1 :=& \delta_u^n + \beta_w^n + \gamma_u^n + \xi_u^n + \alpha_u^n + \theta_u^n + \zeta_u^n;
\end{aligned}
$$

with β_u^n, γ_w^n, δ_w^n, η_w^n, *and* β_w^n *being independent of the parameter* ε, *while* δ_u^n, γ_u^n, ξ_u^n, α_u^n, θ_u^n, *and* ζ_u^n *are dependent on* ε. *More specifically, they are given as follows*

$$
\begin{aligned}
\beta_u^n :=& \left\|\frac{\tau_n^2}{8}\cdot\partial_n^2 u_h\right\|_{-1}; \\
\gamma_w^n :=& \left\|\frac{Aw_h^n - Aw_h^{n-1}}{2}\right\|_{-1}; \\
\delta_w^n :=& \left\|w_h^n - w_h^{n-1}\right\|_{-1} + \left\|\frac{\tau_n^2}{8}\partial_n^2 w_h\right\|_{-1}; \\
\eta_w^n :=& \left\|(Aw_h^{n-1} + w_h^{n-1}) - (Aw_h^n + w_h^n)\right\|_{-1} + \left\|\frac{\tau_n^2}{8}\partial_n^2(Aw_h + w_h)\right\|_{-1}; \\
\delta_u^n :=& \left\|\frac{u_h^n - u_h^{n-1}}{\varepsilon}\right\|; \\
\beta_w^n :=& \left\|\frac{w_h^n - w_h^{n-1}}{2}\right\|; \\
\gamma_u^n :=& \varepsilon\left\|\frac{Au_h^n - Au_h^{n-1}}{2}\right\|; \\
\xi_u^n :=& \left\|\frac{Pf(u_h^n) - Pf(u_h^{n-1})}{2\varepsilon}\right\|; \\
\alpha_u^n :=& \frac{1}{\varepsilon}C\left(\mathcal{E}_u^n + \mathcal{E}_u^{n-1} + \mathcal{E}_u^{n-2}\right); \\
\theta_u^n :=& 2\left\|\left(\varepsilon Au_h^{n-1} + \frac{1}{\varepsilon}h(u_h^{n-1}) - w_h^{n-1}\right) - \left(\varepsilon Au_h^n + \frac{1}{\varepsilon}h(u_h^n) - w_h^n\right)\right\| \\
&+ \left\|\left(\varepsilon Au_h^{n-1} + \frac{1}{\varepsilon}h(u_h^{n-1}) - w_h^{n-1}\right) - \left(\varepsilon Au_h^{n-2} + \frac{1}{\varepsilon}h(u_h^{n-2}) - w_h^{n-2}\right)\right\|; \\
\zeta_u^n :=& \left\|\frac{3(u_h^n)^2u_h^{n-1} - 2(u_h^n)^3 - (u_h^{n-1})^3}{\varepsilon}\right\| + \left\|\frac{3u_h^n(u_h^{n-1})^2 - 2(u_h^{n-1})^3 - (u_h^n)^3}{\varepsilon}\right\| \\
&+ \left\|\frac{\left(3(u_h^n)^2\partial_n^2 u_h - 3u_h^n u_h^{n-1}\partial_n^2 u_h\right)\tau_n^2}{8\varepsilon}\right\| + \left\|\frac{\left(3(u_h^{n-1})^2\partial_n^2 u_h - 3u_h^n u_h^{n-1}\partial_n^2 u_h\right)\tau_n^2}{8\varepsilon}\right\|
\end{aligned}
$$

$$+\left\|\frac{\left(3u_h^n u_h^{n-1}\partial_n^2 u_h - \frac{\frac{(u_h^n)^3-(u_h^{n-1})^3}{\tau_n}-\frac{(u_h^{n-1})^3-(u_h^{n-2})^3}{\tau_{n-1}}}{\frac{\tau_n+\tau_{n-1}}{2}}\right)\tau_n^2}{8\varepsilon}\right\|$$

$$+\left\|\frac{\left(3u_h^n(\partial_n^2 u_h)^2 - 3u_h^{n-1}(\partial_n^2 u_h)^2\right)\tau_n^4}{64\varepsilon}\right\| + \left\|\frac{\left(3u_h^{n-1}(\partial_n^2 u_h)^2\right)\tau_n^4}{64\varepsilon}\right\| + \left\|\frac{(\partial_n^2 u_h)^3\tau_n^6}{512\varepsilon}\right\|,$$

here C_S, C are constants, which are independent of mesh size, and $\mathcal{E}_u^n := \mathcal{E}[u_h^n]$ is defined as (2.25).

The proof of this theorem is provided in "Appendix A".

Remark 3.1 The a posteriori error estimator in Theorem 3.2 can be divided into two categories. The terms γ_w^n, β_u^n, η_w^n, δ_w^n, δ_u^n, γ_u^n, ξ_u^n, β_w^n, θ_u^n, ζ_u^n are viewed as the a posteriori error indicators for time discretization, the terms $\widetilde{\mathcal{E}_u^n}$ and α_u^n are the spatial discretization error indicators.

Remark 3.2 As stated in [5], the bounds of the error, which only depend on ε^{-1} in a polynomial, provide that the integral of $\Lambda_{AC}(t)$ over $(0, T)$ grows at most logarithmically in ε^{-1} and this can be monitored numerically. From an analytical point of view, our results prove stability with polynomial dependence on ε^{-1} for solutions of (1.1).

3.2 Adaptive Algorithm

In view of the a posteriori error estimator of Theorem 3.2, we design the algorithms for time-step size control and spatial adaptation in this part.

We adjust the time-step size in view of the error equidistribution strategy, which means that the time discretization error should be evenly distributed to each time interval $(t_{n-1}, t_n]$, $n = 1, 2, \ldots, N$. Let TOL_{time} be the tolerance allowed for the part of the a posteriori error estimator in (3.9) related to the time discretization, that is,

$$\sum_{n=1}^{N}\tau_n(\gamma_w^n+\beta_u^n+\eta_w^n+\delta_w^n+\delta_u^n+\gamma_u^n+\xi_u^n+\beta_w^n+\theta_u^n+\zeta_u^n)^2 \le TOL_{time}. \quad (3.10)$$

Generally, we can achieve (3.10) by adjusting the time-step size τ_n so as to have the following relations

$$\eta_{time}^n := \gamma_w^n+\beta_u^n+\eta_w^n+\delta_w^n+\delta_u^n+\gamma_u^n+\xi_u^n+\beta_w^n+\theta_u^n+\zeta_u^n \le \sqrt{TOL_{time}/T} := TOL_t. \quad (3.11)$$

We summarize the procedure of time-step size control in Algorithm 1.

Let TOL_{space} be the tolerance allowed for the part of the a posteriori error estimator in (3.9) related to the spatial discretization. For the recovery type error estimator, we adopt the SCR-based error estimator. The SCR gradient recovery method was proposed by Huang and Yi [31, 46], it can produce a superconvergent recovered gradient, which in turn provides the SCR-based error estimator that is asymptotically exact. Similar to time discretization, we aim to achieve the following relation at each time step n,

$$\eta_{space}^n := \widetilde{\mathcal{E}_u^n} + \alpha_u^n \le \sqrt{TOL_{space}/T} := TOL_s. \quad (3.12)$$

Algorithm 1 Time-step size control

Given tolerances $TOL_t, TOL_{t,m} := \sqrt{TOL_{time,min}/T}$, parameters $\delta_1 \in (0,1), \delta_2 > 1$;
Set $\tau_n := \tau_{n-1}, t_n := t_{n-1} + \tau_n$;
Solve the discrete problem and compute the time error estimator η^n_{time};
while $\eta^n_{time} > TOL_t$ or $\eta^n_{time} < TOL_{t,m}$ **do**
  if $\eta^n_{time} > TOL_t$ **then**
    Set $\tau_n := \delta_1 \cdot \tau_n$ and $t_n := t_{n-1} + \tau_n$;
  else
    Set $\tau_n := \delta_2 \cdot \tau_n$ and $t_n := t_{n-1} + \tau_n$;
  end if
  Solve the discrete problem and compute the time error estimator η^n_{time};
end while

Given the refinement and the coarsening parameters TOL_r, TOL_c, respectively, we adopt the following Maximum mark strategy to mark the elements for refinement or coarsening. Set

$$\eta^n_K := \left\| G^n u^n_h - \nabla u^n_h \right\|_K, \ \eta^n_{\max} := \max\{\eta^n_K, K \in \mathcal{T}^n_h\}, \tag{3.13}$$

choose the elements $\{K : \eta^n_K > TOL_r \times \eta^n_{\max}\}$ for refinement, and choose the elements $\{K : \eta^n_K < TOL_c \times \eta^n_{\max}\}$ for coarsening.

In view of the error indicators above, we design the following time-space adaptive algorithm for Cahn–Hilliard equation, which is outlined in Algorithm 2.

4 Numerical Examples

In this section, we present three examples to demonstrate the reliability and effectiveness of the proposed adaptive algorithm based on the a posteriori error estimator of Theorem 3.2. In Example 4.1, we investigate the main part of the space and time discretization error indicators numerically. In Example 4.2, we focus on illustrating the efficiency of the a posteriori error estimator based on the recovery type and the necessity of time-space adaptation by comparing them with the residual type and space-only adaptation, respectively. We provide the corresponding numerical results, including the discrete energy history, the change in the number of nodes and time steps, the numerical solutions, adaptive meshes, and CPU time, to support our conclusions. For the last example, we apply the proposed time-space adaptive algorithm to the three-dimensional Cahn–Hilliard equation.

In all examples, we take the parameters

$$\delta_1 = \frac{1}{2}, \qquad \delta_2 = 2,$$

and the remaining parameters will be specified in each example.

Example 4.1 Consider the Cahn–Hilliard equation (2.2) with the initial condition

$$u_0(x,y) = \tanh\left(\left((x-0.3)^2 + y^2 - 0.25^2\right)/\varepsilon\right) \tanh\left(\left((x+0.3)^2 + y^2 - 0.3^2\right)/\varepsilon\right),$$

where $\Omega = [-1,1]^2$ and the parameters $\varepsilon = 0.01$, $TOL_t = 50$, $TOL_{t,m} = 5$, $TOL_s = 10$, $TOL_i = 0.002$.

We apply the proposed time-space adaptive algorithm to solve the Cahn–Hilliard equation, the numerical solutions of u and the corresponding adaptive meshes are shown in Fig. 1,

Algorithm 2 Time-space adaptive algorithm for the Cahn–Hilliard equation

Given $TOL_t, TOL_{t,m}, TOL_s, TOL_i, \delta_1 \in (0,1), \delta_2 > 1$;
Given the initial time step τ_0, initial mesh $\mathcal{T}_h^0$, and initial solution u_h^0;
Set $n = 0$, $t_0 = 0$, $E(u_h^{-1}) = 0$;
Compute the initial error estimator $\eta^0_{initial} = \|u_0 - u_h^0\|$;
Refine $\mathcal{T}_h^0$ to get a mesh such that $\eta^0_{initial} \le TOL_i$;
Compute the energy $E(u_h^0)$;
while $E(u_h^n) - E(u_h^{n-1}) > TOL_e$ **do**
    Set $n := n+1$, $\mathcal{T}_h^n := \mathcal{T}_h^{n-1}$, $\tau_n := \tau_{n-1}$, $t_n := t_{n-1} + \tau_n$;
    Solve the discrete problem and compute the time error estimator η^n_{time};
    while $\eta^n_{time} > TOL_t$ or $\eta^n_{time} < TOL_{t,m}$ **do**
        if $\eta^n_{time} > TOL_t$ **then**
            Set $\tau_n := \delta_1 \cdot \tau_n$ and $t_n := t_{n-1} + \tau_n$;
        else
            Set $\tau_n := \delta_2 \cdot \tau_n$ and $t_n := t_{n-1} + \tau_n$;
        end if
        Solve the discrete problem and compute the time error estimator η^n_{time};
    end while
    Compute the space error estimator η^n_{space}, η^n_K and $\eta^n_{\max}$;
    while $\eta^n_{space} > TOL_s$ **do**
        Mark elements for refinement;
        Refine mesh $\mathcal{T}_h^n$ to generate a new mesh $\mathcal{T}_h^n$;
        Solve the discrete problem for u_h^n on the new mesh $\mathcal{T}_h^n$ using data u_h^{n-1};
        Compute the time error estimator η^n_{time};
        while $\eta^n_{time} > TOL_t$ or $\eta^n_{time} < TOL_{t,m}$ **do**
            if $\eta^n_{time} > TOL_t$ **then**
                Set $\tau_n := \delta_1 \cdot \tau_n$ and $t_n := t_{n-1} + \tau_n$;
            else
                Set $\tau_n := \delta_2 \cdot \tau_n$ and $t_n := t_{n-1} + \tau_n$;
            end if
            Solve the discrete problem and compute the time error estimator η^n_{time};
        end while
        Compute the space error estimator η^n_{space}, η^n_K and $\eta^n_{\max}$;
    end while
    Compute the energy $E(u_h^n)$;
    Mark elements for coarsen and coarsen $\mathcal{T}_h^n$ producing a modified mesh $\mathcal{T}_h^n$;
end while

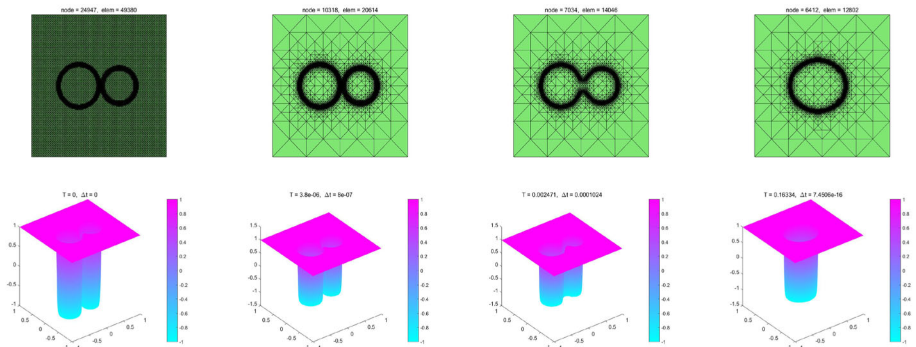

Fig. 1 Example 4.1, First line: adaptive meshes; Second line: snapshots of numerical solutions for u

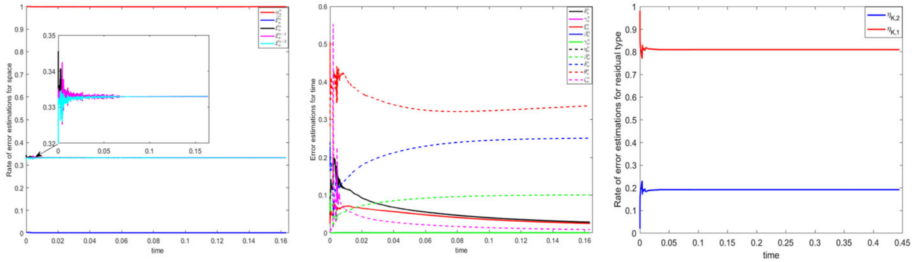

Fig. 2 Example 4.1. Left: Error indicators for spatial discretization of recovery type; Middle: Error indicators for time discretization of recovery type; Right: Error indicators for spatial discretization of residual type

respectively. From the pictures, we can see that the meshes follow the zeros level set of u as it moves.

From Theorem 3.2, the proposed error estimator contains twelve terms,

$$\eta_{time}^n = \gamma_w^n + \beta_u^n + \eta_w^n + \delta_w^n + \delta_u^n + \gamma_u^n + \xi_u^n + \beta_w^n + \theta_u^n + \zeta_u^n,$$
$$\eta_{space}^n = \widetilde{\mathcal{E}}_u^n + \alpha_u^n.$$

We numerically investigate which terms are the main part of the time and space discretization error indicators. We also test the performance of the residual type error estimator provided in [21], in which the local error estimators are defined by

$$\eta_{K,j}(t) = h_K \|R_{K,j}\|_{L^2(K)} + \sum_{\tau \in \partial K} \left(\frac{1}{2} h_\tau \|J_{\tau,j}\|^2_{L^2(\tau)} \right)^{\frac{1}{2}}, \quad j = 1, 2, \tag{4.1}$$

with the element residual

$$\begin{aligned} R_{K,1} &= u_{h,t}|_K + \mathcal{A}(w_h(t)|_K), \\ R_{K,2} &= \mathcal{A}(u_h(t)|_K) + \frac{1}{\varepsilon^2} f(u_h(t)|_K) - \frac{1}{\varepsilon} w_h(t)|_K, \end{aligned} \tag{4.2}$$

and the residual jumps across τ

$$\begin{aligned} J_{\tau,1}(t) &= \left(\nabla w_h(t)|_{K_1} - \nabla w_h(t)|_{K_2} \right) \cdot \mathbf{n}, \\ J_{\tau,2}(t) &= \left(\nabla u_h(t)|_{K_1} - \nabla u_h(t)|_{K_2} \right) \cdot \mathbf{n}, \end{aligned} \tag{4.3}$$

here $\mathbf{n}$ is the unit normal vector to τ pointing from K_1 to K_2. The corresponding total spatial discretization error estimator is taken as

$$\eta(t) = \left(\sum_{K \in \mathcal{T}_h} \left(\eta_{K,1}^2(t) + \eta_{K,2}^2(t) \right) \right)^{\frac{1}{2}}. \tag{4.4}$$

Figure 2 plots each parts of the error indicators. It shows that: i) for the recovery type error indicator, the time discretization error estiamtor η_{time}^n is dominated by θ_u^n, and the space discretization error estimator η_{space}^n is dominated by $\mathcal{E}_u^n$; ii) $\eta_{K,1}(t^n)$ is the main part of the residual type error indicator $\eta(t^n)$. In the following examples, we adopt θ_u^n as the time discretization error indicator, and $\mathcal{E}_u^n$ or $\eta_{K,1}(t^n)$ as the spatial discretization error indicator, respectively.

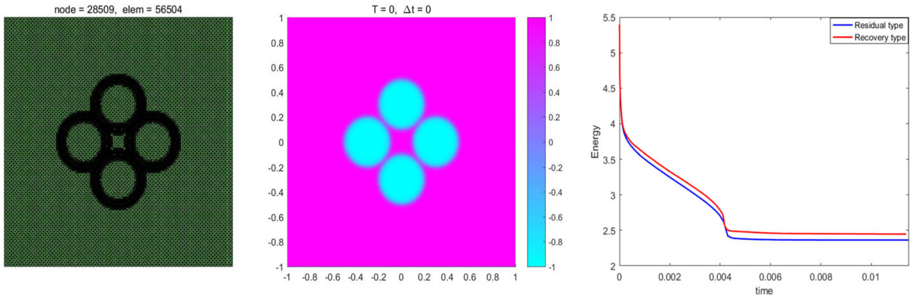

Fig. 3 Example 4.2, Left: initial mesh; Middle: the contour plot of u_0; Right: discrete energy

Table 1 Example 4.2 (T = 0.01), CPU time for two kinds of types by using time-space adaptive algorithm and space-only adaptation, respectively (11th Gen Intel(R) Core(TM) i5-1135G7 @ 2.40GHz 2.42GHz)

CPU time	Time-space adaptation	Space-only adaptation
Recovery type	389 s	1095 s
Residual type	106975 s	–

Example 4.2 Consider the model equation (2.2) with the parameters $\Omega = [-1, 1]^2$, $\varepsilon = 0.01$, $TOL_t = 50$, $TOL_{t,m} = 5$, $TOL_s = 4$, $TOL_i = 0.002$ and the initial condition

$$u_0(x, y) = \tanh\left(\left((x-0.3)^2 + y^2 - 0.2^2\right)/\varepsilon\right) \tanh\left(\left((x+0.3)^2 + y^2 - 0.2^2\right)/\varepsilon\right) \times \tanh\left(\left(x^2 + (y-0.3)^2 - 0.2^2\right)/\varepsilon\right) \tanh\left(\left(x^2 + (y+0.3)^2 - 0.2^2\right)/\varepsilon\right).$$

In this example, we compare the recovery type a posteriori error estimator with the residual type. Figure 3 displays the initial mesh, contour plot of the initial numerical solution, and discrete energy history for the two spatial error estimators based on the proposed time-space adaptive algorithm. We can see clearly that the energy decreases over time. Figure 4 shows the sequences of adaptive meshes and contour plots of the corresponding approximate solutions produced by the time-space adaptive algorithm guided by the recovery and residual type error indicators for the spatial discretization, respectively. The adaptive meshes match the numerical solutions of Algorithm 2 based on the recovery type error indicator better than the residual type. The corresponding time-step and number of nodes are also displayed in Fig. 5. We observe that as the time-step grows, the degree of freedom based on the recovery type is much less than the residual type, indicating that the recovery type a posteriori error estimation is clearly superior to the residual type.

Furthermore, we evaluate the efficiency of the adaptive algorithm with time and space adaptation. Table 1 reports the corresponding CPU time. We observe that: (i) the time-space adaptive method based on our proposed recovery type error estimator is significantly more efficient than the adaptive method based on the residual type error indicator; (ii) the time-space adaptation is more efficient than the adaptive method with space-only adaptation.

Example 4.3 In the last example, we consider the three dimensional Cahn–Hilliard equation (2.2) with the following initial condition

$$u_0(x, y, z) = \varepsilon \cos(1.5\pi x) \cos(1.5\pi y)\big(\sin(\pi z) + \sin(2\pi z)\big),$$

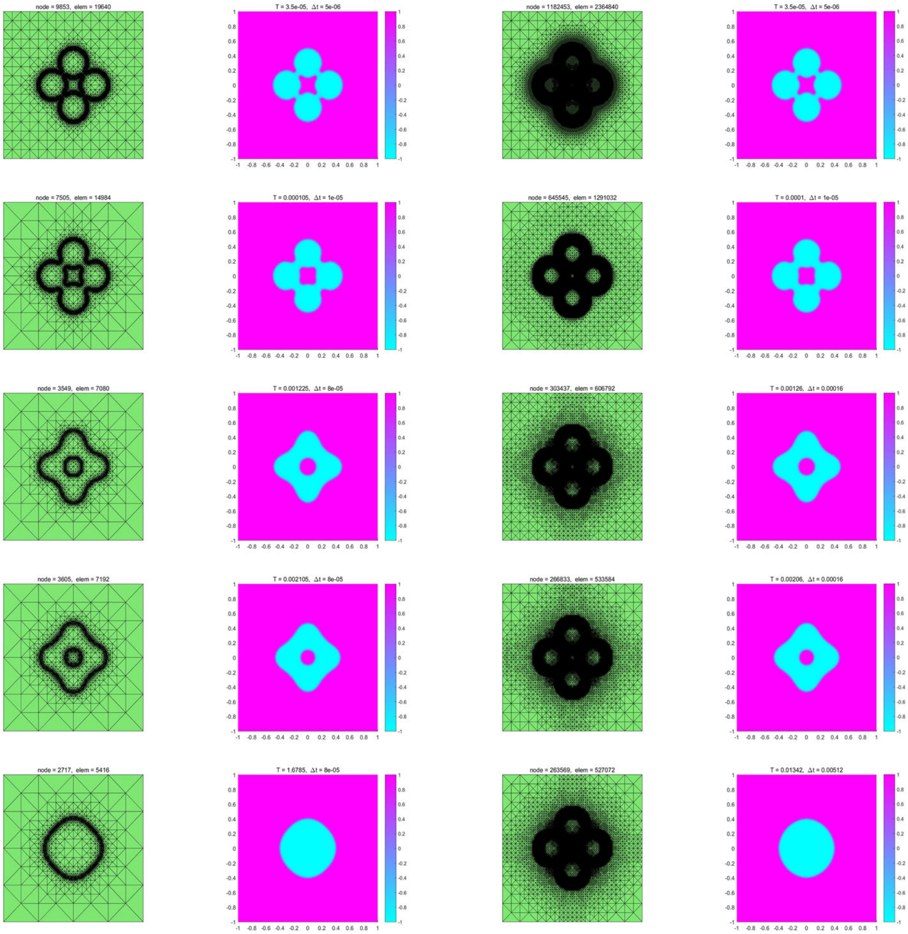

Fig. 4 Example 4.2, adaptive meshes and snapshots of numerical solutions; First and second column: recovery type; Third and fourth column: residual type

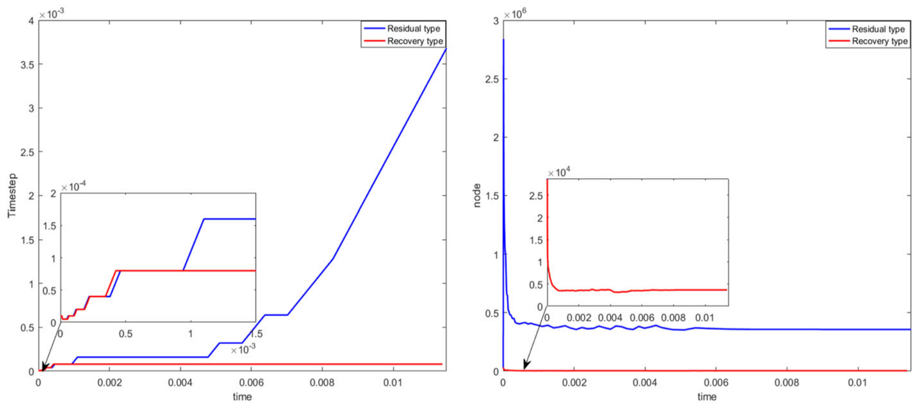

Fig. 5 Example 4.2, Left: time-steps; Right: number of nodes

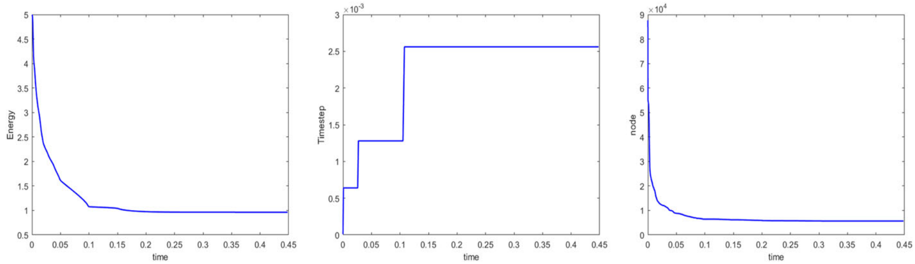

Fig. 6 Example 4.3, Left: discrete energy; Middle: time-steps; Right: number of nodes

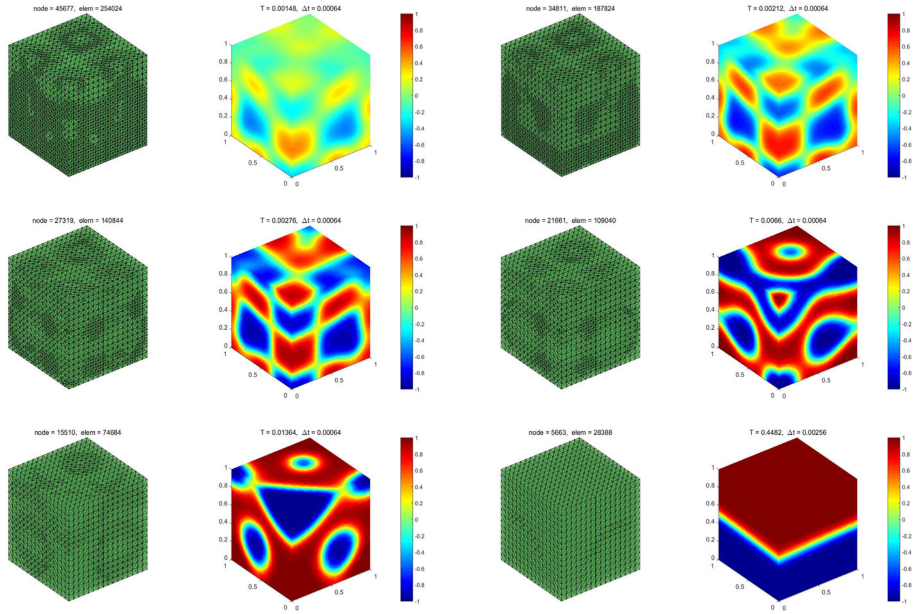

Fig. 7 Example 4.3, adaptive meshes and snapshots of numerical solutions

where $\Omega = [-1, 1]^3$ and the parameters $\varepsilon = 0.05, TOL_t = 20, TOL_{t,m} = 1, TOL_s = 1.5, TOL_i = 8e - 5$.

Figure 6 displays the contour plots of the discrete energy history, time steps, and the change in the number of nodes with time. It is evident that the energy and the number of nodes both decrease over time, and the time steps change with time. In Fig. 7, we show the sequence of adaptive meshes and contour plots of the corresponding approximate solutions. We observe that the meshes adapt around the zero level set, which confirms the effectiveness of the derived a posteriori error estimation and adaptive algorithm for the three-dimensional Cahn–Hilliard equation.

5 Conclusions

In this paper, we derived a novel SCR-based recovery type a posteriori error estimator for the Crank–Nicolson finite element method applied to the Cahn–Hilliard equation. The derivation of the error estimator utilized the elliptic reconstruction technique and the time reconstruction technique, which was based on approximations on three time levels and led to a second order error estimator for time discretization. Based on the derived a posteriori error estimator, we designed an efficient time-space adaptive algorithm. The numerical results indicated that the recovery-type a posteriori error estimator and the time-space adaptive strategy could greatly improve the efficiency of the adaptive algorithm for the Cahn–Hilliard equation. Notably, our proposed time-space adaptive finite element method outperformed the adaptive finite element method based on residual-type a posteriori error estimators, as well as the space-only adaptive finite element method. These results demonstrate the superior efficiency of our method in accurately solving the Chan–Hilliard equation at hand.

Acknowledgements The authors express their sincere thanks to the referees for their useful comments and suggestions, which led to improvements of the presentation in this paper.

Funding Chen's research was supported by NSFC Project (12201010), Natural Science Research Project of Higher Education in Anhui Province (2022AH040027). Huang's research was partially supported by NSFC Project (11971410) and China's National Key R&D Programs (2020YFA0713500). Yi's research was partially supported by NSFC Project (12071400, 12261131501) and Hunan Provincial NSF Project (2021JJ40189). Yin's research was supported by the University of Texas at El Paso Startup Award.

Data availability Enquiries about data availability should be directed to the authors.

Declarations

Conflict of interest The authors declare that they have no conflict of interest.

Appendix A. Proof of Theorem 3.2

In this section, we present the proof of the Theorem 3.2. To begin with, we recall the following results.

Lemma A.1 [3] *Let* $\dot{V} := \left\{\phi \in H^1(\Omega), \bar{\phi} := \frac{1}{|\Omega|}\int_\Omega \phi dx = 0\right\}$, *there exists* $C_I > 0$ *such that for all* $\phi \in \dot{V}$ *if* $d = 2$ *and for all* $\phi \in \dot{V} \cap L^\infty(\Omega)$ *if* $d = 3$, *we have*

$$\|\phi\|^3_{L^3(\Omega)} \le C_I \|\phi\|^{1-\sigma}_{L^\infty(\Omega)} \|\nabla\Delta^{-1}\phi\|^\sigma \|\nabla\phi\|^2, \tag{A.1}$$

where $\sigma = 1$ *if* $d = 2$ *and* $\sigma = \frac{4}{5}$ *if* $d = 3$.

Lemma A.2 [5] (Generalized Gronwall's Lemma) *Suppose that the nonnegative functions* $y_1 \in C([0, T])$, y_2, $y_3 \in L^1(0, T)$, $a \in L^\infty(0, T)$, *and the real number* $A \ge 0$ *satisfy*

$$y_1(t) + \int_0^t y_2(s)ds \le A + \int_0^t a(s)y_1(s)ds + \int_0^t y_3(s)ds$$

for all $t \in [0, T]$. *Assume that for* $B \ge 0$, $\beta \ge 0$ *and every* $t \in [0, T]$, *we have*

$$\int_0^t y_3(s)ds \le B \sup_{s\in[0,t]} y_1^\beta(s) \int_0^t (y_1(s) + y_2(s))\, ds.$$

Setting $E := exp\left(\int_0^T a(s)ds\right)$ *and assume that* $8AE \le (8B(1+T)E)^{-1/\beta}$*, then we obtain*

$$\sup_{t\in[0,T]} y_1(t) + \int_0^T y_2(s)ds \le 8Aexp\left(\int_0^T a(s)ds\right).$$

To prove Theorem 3.2, we introduce the L^2 lifting property for the nonlinear elliptic problem (2.10b). This is inspired by the L^2 lifting property for a similar nonlinear elliptic problem discussed in [26]:

$$\begin{cases} -\Delta z + b(x,z) = 0, & \text{in } \Omega \times (0,T], \\ u = 0, & \text{on } \partial\Omega \times [0,T], \end{cases} \tag{A.2}$$

where the nonlinear term b satisfies

$$\sup_{x\in\bar{\Omega}} \left| b(x,z) - b(x,z_0) + \frac{\partial b}{\partial z}(x,z_0)(z_0 - z) \right| \lesssim (1 + \max\{|z|^s, |z_0|^s\})|z - z_0|^q, \\ \forall z,\ z_0 \in R, \tag{A.3}$$

for $q \in (1,2],\ s \in [0, 5-q]$.

Lemma A.3 (L^2 lifting property) *Given* $h_0 \ll 1$. *For the nonlinear elliptic problem (2.10b), if* $h = \max\{h_K, K \in \mathcal{T}_h\} \in (0, h_0]$, *then*

$$\|\mu - \mu_h\| \le \kappa(h)\|\mu - \mu_h\|_{1,\Omega}, \tag{A.4}$$

where $\kappa(h) = C_I C_R h^s + \frac{1}{\varepsilon^2}\hat{C}_I C_R h^s$, *here* $C_R,\ C_I,\ \hat{C}_I$ *are constants independent of* ε *and* h.

Proof Let $\omega \in H^{1+s}(\Omega)$ for some $0 < s \le 1$ be the solution to the dual problem of (2.10b): Find $\omega \in H^1(\Omega)$, such that

$$\varepsilon a(\omega, v) + \langle \mathfrak{B}(\mu,\mu_h)\omega, v\rangle = \langle \mu - \mu_h, v\rangle, \qquad \forall v \in H^1(\Omega), \tag{A.5}$$

where the operator

$$\mathfrak{B}(\mu,\mu_h) = \frac{1}{\varepsilon}\int_0^1 3[\mu_h + \xi(\mu-\mu_h)^2]d\xi.$$

Obviously, it holds that

$$\frac{1}{\varepsilon}\left(\mu^3 - \mu_h^3\right) = \mathfrak{B}(\mu,\mu_h)(\mu-\mu_h). \tag{A.6}$$

By the regularity estimate [23, 24, 35] for the dual problem (A.5),

$$|\omega|_{H^{1+s}(\Omega)} \le \frac{1}{\varepsilon}C_R\|\mu-\mu_h\|_{0,\Omega}. \tag{A.7}$$

Let $I^h : H^1(\Omega) \to V_h$ be a quasi-interpolator, satisfying

$$\|\omega - I^h\omega\|_{1,\Omega} \le C_I h^s |\omega|_{H^{1+s}}, \tag{A.8}$$

$$\|\omega - I^h\omega\|_{0,\Omega} \le \hat{C}_I h^s |\omega|_{H^{1+s}}. \tag{A.9}$$

Consider the linearized dual problem (A.5) with $v = \mu - \mu_h \in H^1(\Omega)$, we obtain

$$\varepsilon a(\mu-\mu_h, \omega) + \langle \mathfrak{B}(\mu,\mu_h)(\mu-\mu_h), \omega\rangle = \|\mu-\mu_h\|^2. \tag{A.10}$$

By Galerkin orthogonality, for $I^h\omega \in V_h$,

$$\varepsilon a(\mu - \mu_h, I^h\omega) + \langle \mathfrak{B}(\mu, \mu_h)(\mu - \mu_h), I^h\omega\rangle = 0. \tag{A.11}$$

Subtracting (A.11) from (A.10) and using (A.6), we have

$$\varepsilon a(\mu - \mu_h, \omega - I^h\omega) + \frac{1}{\varepsilon}\langle \mu^3 - \mu_h^3, \omega - I^h\omega\rangle = \|\mu - \mu_h\|^2. \tag{A.12}$$

By using the Cauchy-Schwarz inequality, interpolation estimate (A.8) and regularity (A.7) for the first term on the left hand side (LHS) of (A.12), it holds

$$\begin{aligned} \left|\varepsilon a(\mu - \mu_h, \omega - I^h\omega)\right| &= \left|\varepsilon \left((\nabla(\mu - \mu_h), \nabla(\omega - I^h\omega)\right)\right| \\ &\le \varepsilon\|\nabla(\mu - \mu_h)\| \cdot \|\nabla(\omega - I^h\omega)\| \\ &\le \varepsilon\|\mu - \mu_h\|_{1,\Omega} \cdot \|\omega - I^h\omega\|_{1,\Omega} \\ &\le \varepsilon C_I h^s\|\mu - \mu_h\|_{1,\Omega} \cdot |\omega|_{H^{1+s}} \\ &\le C_I h^s C_R\|\mu - \mu_h\|_{1,\Omega} \cdot \|\mu - \mu_h\|_{0,\Omega}. \end{aligned} \tag{A.13}$$

For the second term on LHS of (A.12), applying the Cauchy-Schwarz inequality, we have

$$\begin{aligned} \left|\frac{1}{\varepsilon}\left\langle \mu^3 - \mu_h^3, \omega - I^h\omega\right\rangle\right| &= \left|\frac{1}{\varepsilon}\left\langle (\mu - \mu_h)(\mu^2 + \mu\mu_h + \mu_h^2), \omega - I^h\omega\right\rangle\right| \\ &\le \frac{1}{\varepsilon}\|\mu - \mu_h\|_{0,p,\Omega} \cdot \|\mu^2 + \mu\mu_h + \mu_h^2\|_{0,q,\Omega} \cdot \|\omega - I^h\omega\|_{0,k,\Omega} \end{aligned} \tag{A.14}$$

with $\frac{1}{p} + \frac{1}{q} + \frac{1}{k} = 1$. Taking $p = q = 4,\ k = 2$ in (A.14), and using embedding theorem, interpolation estimate (A.9) and regularity (A.7) give

$$\begin{aligned} \left|\frac{1}{\varepsilon}\left\langle \mu^3 - \mu_h^3, \omega - I^h\omega\right\rangle\right| &\le \frac{1}{\varepsilon}\|\mu - \mu_h\|_{0,4,\Omega} \cdot \|\mu^2 + \mu\mu_h + \mu_h^2\|_{0,4,\Omega} \cdot \|\omega - I^h\omega\|_{0,2,\Omega} \\ &\le \frac{1}{\varepsilon}\|\mu - \mu_h\|_{1,\Omega} \cdot \|\mu^2 + \mu\mu_h + \mu_h^2\|_{1,\Omega} \cdot \|\omega - I^h\omega\|_{0,\Omega} \\ &\le \frac{1}{\varepsilon}\hat{C}_I h^s\|\mu - \mu_h\|_{1,\Omega} \cdot |\omega|_{H^{1+s}} \\ &\le \frac{1}{\varepsilon^2}\hat{C}_I C_R h^s\|\mu - \mu_h\|_{1,\Omega} \cdot \|\mu - \mu_h\|_{0,\Omega}. \end{aligned} \tag{A.15}$$

Plugging (A.13) and (A.15) into (A.12) gives

$$\begin{aligned} \|\mu - \mu_h\|^2 \le C_I h^s C_R\|\mu - \mu_h\|_{1,\Omega} \cdot \|\mu - \mu_h\|_{0,\Omega} + \frac{1}{\varepsilon^2}\hat{C}_I C_R h^s\|\mu \\ - \mu_h\|_{1,\Omega} \cdot \|\mu - \mu_h\|_{0,\Omega}. \end{aligned}$$

Thus, the result of (A.4) is obtained by simplification. □

Now, we are ready to present the proof of Theorem 3.2.

Proof According to (3.7), we have that

$$\partial_t e_u + \mathcal{A}e_w = -\mathcal{A}\epsilon_w + \frac{Aw_h^n - Aw_h^{n-1}}{2} + \mathcal{A}(q(t) - q^n) + w_h^n - Rw_h^n + (t - t_{n-\frac{1}{2}})\partial_n^2 u_h, \tag{A.16}$$

$$
\begin{aligned}
\varepsilon \mathcal{A} e_u - e_w =& - \varepsilon \mathcal{A} \epsilon_u + \epsilon_w + \varepsilon \frac{A u_h^n - A u_h^{n-1}}{2} + \frac{P f(u_h^n) - P f(u_h^{n-1})}{2\varepsilon} - \frac{w_h^n - w_h^{n-1}}{2} \\
&+ \varepsilon \mathcal{A}(p(t) - p^n) - (q(t) - q^n) + \frac{f(u) - f(p^n)}{\varepsilon} + \frac{1}{\varepsilon}\left(u_h^n - p^n\right).
\end{aligned} \tag{A.17}
$$

To make the conclusion clean, we separate the remaining of this proof into eleven steps.

Step 1: Multiplying both sides of (A.16) by $-\Delta^{-1} e_u$ and (A.17) by e_u, respectively, then adding the resulting equations, we obtain

$$
\begin{aligned}
&\frac{1}{2}\frac{d}{dt}\|\nabla \Delta^{-1} e_u\|^2 + \varepsilon \|\nabla e_u\|^2 = \left(\frac{A w_h^n - A w_h^{n-1}}{2}, -\Delta^{-1} e_u\right) + \left(\mathcal{A}(q(t) - q^n), -\Delta^{-1} e_u\right) \\
&\quad + \left(w_h^n - R w_h^n, -\Delta^{-1} e_u\right) + \left((t - t_{n-\frac{1}{2}})\partial_n^2 u_h, -\Delta^{-1} e_u\right) \\
&\quad - \varepsilon a\left(\epsilon_u, e_u\right) + \varepsilon \left(\frac{A u_h^n - A u_h^{n-1}}{2}, e_u\right) + \frac{1}{\varepsilon}\left(u_h^n - p^n, e_u\right) \\
&\quad + \left(\frac{P f(u_h^n) - P f(u_h^{n-1})}{2\varepsilon}, e_u\right) + \left(-\frac{w_h^n - w_h^{n-1}}{2}, e_u\right) \\
&\quad + \left(\left(\varepsilon \mathcal{A}\left(p(t) - p^n\right) - \frac{1}{\varepsilon}\left(f(p^n)\frac{t_n - t}{\tau_n} - f(p^{n-1})\frac{t_n - t}{\tau_n}\right) - (q(t) - q^n)\right), e_u\right) \\
&\quad + \left(\frac{1}{\varepsilon}\left(f(u_h^n)\frac{t - t_{n-1}}{\tau_n} + f(u_h^{n-1})\frac{t_n - t}{\tau_n} - f(p^n) + f(p^n)\frac{t_n - t}{\tau_n} - f(p^{n-1})\frac{t_n - t}{\tau_n}\right), e_u\right) \\
&\quad + \left(\frac{1}{\varepsilon}\left(f(u_h) - f(u_h^n)\frac{t - t_{n-1}}{\tau_n} - f(u_h^{n-1})\frac{t_n - t}{\tau_n})\right), e_u\right) + \left(\frac{1}{\varepsilon}\left(f(u) - f(u_h)\right), e_u\right),
\end{aligned}
$$

for all $t \in (t_{n-1}, t_n]$ and each $n = 1, 2, \ldots, N$. Then integrate with respect to t, we get

$$
\begin{aligned}
&\frac{1}{2}\|\nabla \Delta^{-1} e_u^N\|^2 + \int_0^T \varepsilon \|\nabla e_u\|^2 dt \\
=&\frac{1}{2}\|\nabla \Delta^{-1} e_u^0\|^2 + \int_0^T \left(\frac{A w_h^n - A w_h^{n-1}}{2}, -\Delta^{-1} e_u\right) dt \\
&+ \int_0^T \left(w_h^n - R w_h^n, -\Delta^{-1} e_u\right) dt + \int_0^T \left((t - t_{n-\frac{1}{2}})\partial_n^2 u_h, -\Delta^{-1} e_u\right) dt \\
&+ \int_0^T \left(\mathcal{A}(q(t) - q^n) + q(t) - q^n, -\Delta^{-1} e_u\right) dt + \int_0^T -\varepsilon a\left(\epsilon_u, e_u\right) dt \\
&+ \int_0^T \left(q^n - q(t) - (w_h^n - w_h), -\Delta^{-1} e_u\right) dt + \int_0^T \left(w_h^n - w_h, -\Delta^{-1} e_u\right) dt \\
&+ \int_0^T \varepsilon \left(\frac{A u_h^n - A u_h^{n-1}}{2}, e_u\right) dt + \int_0^T \frac{1}{\varepsilon}\left(u_h^n - p^n, e_u\right) dt \\
&+ \int_0^T \left(\frac{P f(u_h^n) - P f(u_h^{n-1})}{2\varepsilon}, e_u\right) dt + \int_0^T \left(-\frac{w_h^n - w_h^{n-1}}{2}, e_u\right) dt \\
&+ \int_0^T \left(\left(\varepsilon \mathcal{A}\Big(p(t) - p^n\Big) - \frac{1}{\varepsilon}\Big(h(p^n)\frac{t_n - t}{\tau_n} - h(p^{n-1})\frac{t_n - t}{\tau_n}\right.\right.
\end{aligned}
$$

$$
- \frac{1}{2}(t-t_{n-1})(t-t_n)\frac{\frac{h(p^n)-h(p^{n-1})}{\tau_n}-\frac{h(p^{n-1})-h(p^{n-2})}{\tau_{n-1}}}{\frac{\tau_n+\tau_{n-1}}{2}}\Big) - \Big(q(t)-q^n\Big)\Big), e_u\Big)dt
$$

$$
+ \int_0^T \Big(\frac{1}{\varepsilon}\Big(p^n - p^{n-1} - \Big(u_h^n - u_h^{n-1}\Big)\Big)\frac{t_n - t}{\tau_n} + \frac{1}{2\varepsilon}(t-t_{n-1})(t-t_n)
$$

$$
\Big(\frac{\frac{p^n-p^{n-1}}{\tau_n}-\frac{p^{n-1}-p^{n-2}}{\tau_{n-1}}}{\frac{\tau_n+\tau_{n-1}}{2}} - \frac{\frac{u_h^n-u_h^{n-1}}{\tau_n}-\frac{u_h^{n-1}-u_h^{n-2}}{\tau_{n-1}}}{\frac{\tau_n+\tau_{n-1}}{2}}\Big), e_u\Big)dt
$$

$$
+ \int_0^T \Big(\frac{1}{\varepsilon}\Big(u_h^n - u_h^{n-1}\Big)\frac{t_n - t}{\tau_n}, e_u\Big)dt
$$

$$
+ \int_0^T \Big(\frac{1}{\varepsilon}\Big(f(u_h^n)\frac{t-t_{n-1}}{\tau_n} + f(u_h^{n-1})\frac{t_n-t}{\tau_n} - f(p^n) + f(p^n)\frac{t_n-t}{\tau_n} - f(p^{n-1})\frac{t_n-t}{\tau_n}\Big)
$$

$$
+ \frac{1}{2\varepsilon}(t-t_{n-1})(t-t_n)
$$

$$
\left(\frac{\frac{f(u_h^n)-f(u_h^{n-1})}{\tau_n}-\frac{f(u_h^{n-1})-f(u_h^{n-2})}{\tau_{n-1}}}{\frac{\tau_n+\tau_{n-1}}{2}} - \frac{\frac{f(p^n)-f(p^{n-1})}{\tau_n}-\frac{f(p^{n-1})-f(p^{n-2})}{\tau_{n-1}}}{\frac{\tau_n+\tau_{n-1}}{2}}\right), e_u\Big)dt
$$

$$
\int_0^T \Big(\frac{1}{\varepsilon}\Big(f(u_h) - f(u_h^n)\frac{t-t_{n-1}}{\tau_n} - f(u_h^{n-1})\frac{t_n-t}{\tau_n} - \frac{1}{2}(t-t_{n-1})(t-t_n)
$$

$$
\frac{\frac{f(u_h^n)-f(u_h^{n-1})}{\tau_n}-\frac{f(u_h^{n-1})-f(u_h^{n-2})}{\tau_{n-1}}}{\frac{\tau_n+\tau_{n-1}}{2}}\Big), e_u\Big)dt + \int_0^T \Big(\frac{1}{\varepsilon}\left(f(u)-f(u_h)\right), e_u\Big)dt
$$

$$
:= \frac{1}{2}\|\nabla\Delta^{-1}e_u^0\|^2 + \mathcal{B}_1 + \cdots + \mathcal{B}_{17}, \tag{A.18}
$$

where

$$
\mathcal{B}_1 := \int_0^T \left(w_h^n - Rw_h^n, -\Delta^{-1}e_u\right)dt;
$$

$$
\mathcal{B}_2 := \int_0^T \left(\frac{Aw_h^n - Aw_h^{n-1}}{2}, -\Delta^{-1}e_u\right)dt;
$$

$$
\mathcal{B}_3 := \int_0^T \Big((t-t_{n-\frac{1}{2}})\partial_n^2 u_h, -\Delta^{-1}e_u\Big)dt;
$$

$$
\mathcal{B}_4 := \int_0^T \left(\mathcal{A}(q(t)-q^n) + q(t) - q^n, -\Delta^{-1}e_u\right)dt;
$$

$$
\mathcal{B}_5 := \int_0^T -\varepsilon a\left(\epsilon_u, e_u\right)dt;
$$

$$
\mathcal{B}_6 := \int_0^T \left(q^n - q(t) - (w_h^n - w_h), -\Delta^{-1}e_u\right)dt;
$$

$$
\mathcal{B}_7 := \int_0^T \left(w_h^n - w_h, -\Delta^{-1}e_u\right)dt;
$$

$$
\mathcal{B}_8 := \int_0^T \varepsilon\left(\frac{Au_h^n - Au_h^{n-1}}{2}, e_u\right)dt;
$$

$$\mathcal{B}_9 := \int_0^T \frac{1}{\varepsilon}\left(u_h^n - p^n, e_u\right) dt;$$

$$\mathcal{B}_{10} := \int_0^T \left(\frac{Pf(u_h^n) - Pf(u_h^{n-1})}{2\varepsilon}, e_u\right) dt;$$

$$\mathcal{B}_{11} := -\int_0^T \left(\frac{w_h^n - w_h^{n-1}}{2}, e_u\right) dt;$$

$$\mathcal{B}_{12} := \int_0^T \Bigg(\Big(\varepsilon\mathcal{A}\Big(p(t) - p^n\Big) - \frac{1}{\varepsilon}\Big(h(p^n)\frac{t_n - t}{\tau_n} - h(p^{n-1})\frac{t_n - t}{\tau_n} - \frac{1}{2}(t - t_{n-1})(t - t_n)\frac{\frac{h(p^n)-h(p^{n-1})}{\tau_n} - \frac{h(p^{n-1})-h(p^{n-2})}{\tau_{n-1}}}{\frac{\tau_n+\tau_{n-1}}{2}}\Big) - \Big(q(t) - q^n\Big)\Big), e_u\Bigg)dt;$$

$$\mathcal{B}_{13} := \int_0^T \Bigg(\frac{1}{\varepsilon}\Big(p^n - p^{n-1} - \Big(u_h^n - u_h^{n-1}\Big)\Big)\frac{t_n - t}{\tau_n} + \frac{1}{2\varepsilon}(t - t_{n-1})(t - t_n) \Big(\frac{\frac{p^n - p^{n-1}}{\tau_n} - \frac{p^{n-1}-p^{n-2}}{\tau_{n-1}}}{\frac{\tau_n+\tau_{n-1}}{2}} - \frac{\frac{u_h^n-u_h^{n-1}}{\tau_n} - \frac{u_h^{n-1}-u_h^{n-2}}{\tau_{n-1}}}{\frac{\tau_n+\tau_{n-1}}{2}}\Big), e_u\Bigg)dt;$$

$$\mathcal{B}_{14} := \int_0^T \left(\frac{1}{\varepsilon}\left(u_h^n - u_h^{n-1}\right)\frac{t_n - t}{\tau_n}, e_u\right) dt;$$

$$\mathcal{B}_{15} : = \int_0^T \Bigg(\frac{1}{\varepsilon}\left(f(u_h^n)\frac{t-t_{n-1}}{\tau_n} + f(u_h^{n-1})\frac{t_n-t}{\tau_n} - f(p^n) + f(p^n)\frac{t_n - t}{\tau_n} - f(p^{n-1})\frac{t_n - t}{\tau_n}\right) + \frac{1}{2\varepsilon}(t - t_{n-1})(t - t_n) \left(\frac{\frac{f(u_h^n)-f(u_h^{n-1})}{\tau_n} - \frac{f(u_h^{n-1})-f(u_h^{n-2})}{\tau_{n-1}}}{\frac{\tau_n+\tau_{n-1}}{2}} - \frac{\frac{f(p^n)-f(p^{n-1})}{\tau_n} - \frac{f(p^{n-1})-f(p^{n-2})}{\tau_{n-1}}}{\frac{\tau_n+\tau_{n-1}}{2}}\right), e_u\Bigg)dt;$$

$$\mathcal{B}_{16} := \int_0^T \Bigg(\frac{1}{\varepsilon}\Big(f(u_h) - f(u_h^n)\frac{t - t_{n-1}}{\tau_n} - f(u_h^{n-1})\frac{t_n - t}{\tau_n} - \frac{1}{2}(t - t_{n-1})(t - t_n)\frac{\frac{f(u_h^n)-f(u_h^{n-1})}{\tau_n} - \frac{f(u_h^{n-1})-f(u_h^{n-2})}{\tau_{n-1}}}{\frac{\tau_n+\tau_{n-1}}{2}}\Big), e_u\Bigg)dt;$$

$$\mathcal{B}_{17} := \int_0^T \left(\frac{1}{\varepsilon}\left(f(u) - f(u_h)\right), e_u\right) dt.$$

Next we estimate each of the terms $\{\mathcal{B}_j\}_{j=1,\ldots,17}$, separately.

Step 2: First, the term $\mathcal{B}_1$, which contains a spatial discretization error term, is bounded by using Schwarz inequality, the Nitche technique and interpolation error estimation

$$\begin{aligned}\mathcal{B}_1 &= \int_0^T \left(w_h^n - Rw_h^n, -\Delta^{-1}e_u\right) dt\\ &= \sum_{n=1}^{N}\int_{t_{n-1}}^{t_n} \left(w_h^n - Rw_h^n, -\Delta^{-1}e_u\right) dt\end{aligned}$$

$$\leq \sum_{n=1}^{N} \int_{t_{n-1}}^{t_n} \left\| w_h^n - Rw_h^n \right\| \cdot \left\| \Delta^{-1} e_u \right\| dt$$

$$\leq \sum_{n=1}^{N} \int_{t_{n-1}}^{t_n} C_3 h \left\| w_h^n - Rw_h^n \right\|_{1,\Omega} \left\| \Delta^{-1} e_u \right\| dt. \tag{A.19}$$

While h is small enough, it can be ignored. In the same way, the term $\mathcal{B}_6$ can be also ignored.

Similarly, the time discretization terms $\mathcal{B}_2$ and $\mathcal{B}_3$ can be estimated as

$$\begin{aligned}
\mathcal{B}_2 &= \int_0^T \left(\frac{Aw_h^n - Aw_h^{n-1}}{2}, -\Delta^{-1} e_u \right) dt \\
&\leq \sum_{n=1}^{N} \int_{t_{n-1}}^{t_n} \left\| \frac{Aw_h^n - Aw_h^{n-1}}{2} \right\|_{-1} \cdot \left\| \nabla \Delta^{-1} e_u \right\| dt \\
&:= \sum_{n=1}^{N} \int_{t_{n-1}}^{t_n} \gamma_w^n \left\| \nabla \Delta^{-1} e_u \right\| dt.
\end{aligned} \tag{A.20}$$

$$\begin{aligned}
\mathcal{B}_3 &= \int_0^T \left((t - t_{n-\frac{1}{2}}) \partial_n^2 u_h, -\Delta^{-1} e_u \right) dt \\
&\leq \sum_{n=1}^{N} \int_{t_{n-1}}^{t_n} \left\| \frac{\tau_n^2}{8} \cdot \partial_n^2 u_h \right\|_{-1} \cdot \left\| \nabla \Delta^{-1} e_u \right\| dt \\
&:= \sum_{n=1}^{N} \int_{t_{n-1}}^{t_n} \beta_u^n \left\| \nabla \Delta^{-1} e_u \right\| dt.
\end{aligned} \tag{A.21}$$

Step 3: For the term $\mathcal{B}_4$, based on the definition of elliptic reconstruction, we have

$$\begin{aligned}
\mathcal{B}_4 &= \int_0^T \left(\mathcal{A}(q(t) - q^n) + q(t) - q^n, -\Delta^{-1} e_u \right) dt \\
&= \sum_{n=1}^{N} \int_{t_{n-1}}^{t_n} \Big(\mathcal{A}\Big(\frac{t - t_{n-1}}{\tau_n} q^n + \frac{t_n - t}{\tau_n} q^{n-1} + \frac{1}{2}(t - t_{n-1})(t - t_n) \partial_n^2 q - q^n \Big) \\
&\quad + \Big(\frac{t - t_{n-1}}{\tau_n} q^n + \frac{t_n - t}{\tau_n} q^{n-1} + \frac{1}{2}(t - t_{n-1})(t - t_n) \partial_n^2 q - q^n \Big), -\Delta^{-1} e_u \Big) dt \\
&= \sum_{n=1}^{N} \int_{t_{n-1}}^{t_n} \Big((((\mathcal{A}Rw_h^{n-1} + Rw_h^{n-1}) - (\mathcal{A}Rw_h^n + Rw_h^n)) \frac{t_n - t}{\tau_n} \\
&\quad + \frac{1}{2}(t - t_{n-1})(t - t_n)(\partial_n^2 \mathcal{A}q + \partial_n^2 q)), -\Delta^{-1} e_u \Big) dt \\
&\leq \sum_{n=1}^{N} \int_{t_{n-1}}^{t_n} \left\| (\mathcal{A}Rw_h^{n-1} + Rw_h^{n-1} - (\mathcal{A}Rw_h^n + Rw_h^n)) \frac{t_n - t}{\tau_n} + \frac{\tau_n^2}{8} \partial_n^2 (\mathcal{A}Rw_h + Rw_h) \right\|_{-1} \cdot \\
&\quad \left\| \nabla \Delta^{-1} e_u \right\| dt \\
&\leq \sum_{n=1}^{N} \int_{t_{n-1}}^{t_n} \left(\left\| Aw_h^{n-1} + w_h^{n-1} - (Aw_h^n + w_h^n) \right\|_{-1} + \left\| \frac{\tau_n^2}{8} \partial_n^2 (Aw_h + w_h) \right\|_{-1} \right) \cdot \\
&\quad \left\| \nabla \Delta^{-1} e_u \right\| dt
\end{aligned}$$

$$:=\sum_{n=1}^{N}\int_{t_{n-1}}^{t_n}\eta_w^n\cdot\left\|\nabla\Delta^{-1}e_u\right\|dt. \tag{A.22}$$

Step 4: The term $\mathcal{B}_5$ yields the spatial discretization error, which is bounded as follows

$$\begin{aligned}\mathcal{B}_5&=-\int_0^T\varepsilon a(\epsilon_u,e_u)dt\\&=-\sum_{n=1}^{N}\int_{t_{n-1}}^{t_n}\varepsilon a(\epsilon_u,e_u)dt\\&\le\sum_{n=1}^{N}\int_{t_{n-1}}^{t_n}\varepsilon\|\nabla\epsilon_u\|\cdot\|\nabla e_u\|dt\\&\le\sum_{n=1}^{N}\int_{t_{n-1}}^{t_n}\left(2\varepsilon^{-2}\|\nabla\epsilon_u\|^2+\frac{\varepsilon^4}{8}\|\nabla e_u\|^2\right)dt\\&\le\sum_{n=1}^{N}\int_{t_{n-1}}^{t_n}2\varepsilon^{-2}\|\nabla\epsilon_u\|^2dt+\sum_{n=1}^{N}\int_{t_{n-1}}^{t_n}\frac{\varepsilon^4}{8}\|\nabla e_u\|^2dt,\end{aligned}\tag{A.23}$$

and in view of the triangle inequality and the linearity of the operators G and ∇, we get

$$\begin{aligned}\int_{t_{n-1}}^{t_n}\|\nabla\epsilon_u\|^2dt&=\int_{t_{n-1}}^{t_n}\|\nabla(p-u_h)\|^2dt\\&=\int_{t_{n-1}}^{t_n}\Big\|\nabla\Big(\Big(Ru_h^n-u_h^n\Big)\frac{t-t_{n-1}}{\tau_n}+\Big(Ru_h^{n-1}-u_h^{n-1}\Big)\frac{t_n-t}{\tau_n}\\&\quad+\frac{1}{2}(t-t_{n-1})(t-t_n)(\partial_n^2p-\partial_n^2u_h)\Big)\Big\|^2dt\\&\le\int_{t_{n-1}}^{t_n}\bigg(\big\|\nabla\big(Ru_h^n-u_h^n\big)\big\|^2\Big(\frac{t-t_{n-1}}{\tau_n}\Big)^2+\big\|\nabla\big(Ru_h^{n-1}-u_h^{n-1}\big)\big\|^2\Big(\frac{t_n-t}{\tau_n}\Big)^2\\&\quad+\frac{(t-t_{n-1})^2(t-t_n)^2}{4}\|\partial_n^2\nabla p-\partial_n^2\nabla u_h\|^2\\&\quad+2\big\|\nabla\big(Ru_h^n-u_h^n\big)\big\|\cdot\big\|\nabla\big(Ru_h^{n-1}-u_h^{n-1}\big)\big\|\frac{(t-t_{n-1})(t_n-t)}{\tau_n^2}\\&\quad+2\big\|\nabla\big(Ru_h^n-u_h^n\big)\big\|\cdot\|\partial_n^2\nabla p-\partial_n^2\nabla u_h\|\frac{(t-t_{n-1})^2(t-t_n)}{2\tau_n}\\&\quad+2\big\|\nabla\big(Ru_h^{n-1}-u_h^{n-1}\big)\big\|\cdot\|\partial_n^2\nabla p-\partial_n^2\nabla u_h\|\frac{(t-t_{n-1})(t-t_n)^2}{2\tau_n}\bigg)dt\\&\le C_0^2\bigg((\mathcal{E}_u^n)^2\frac{(t-t_{n-1})^3}{3(t_n-t_{n-1})^2}\Big|_{t_{n-1}}^{t_n}-(\mathcal{E}_u^{n-1})^2\frac{(t_n-t)^3}{3(t_n-t_{n-1})^2}\Big|_{t_{n-1}}^{t_n}\\&\quad+2\mathcal{E}_u^n\mathcal{E}_u^{n-1}\frac{\frac{1}{2}(t_n+t_{n-1})t^2-\frac{1}{3}t^3-t_nt_{n-1}\cdot t}{(t_n-t_{n-1})^2}\Big|_{t_{n-1}}^{t_n}\bigg)\\&\quad+\frac{\tau_n^3}{12}C_0\|\partial_n^2\nabla p-\partial_n^2\nabla u_h\|\Big(\mathcal{E}_u^n+\mathcal{E}_u^{n-1}\Big)+\frac{\tau_n^5}{120}\|\partial_n^2\nabla p-\partial_n^2\nabla u_h\|^2\\&\le\frac{C_0^2}{3}\tau_n\left((\mathcal{E}_u^n)^2+(\mathcal{E}_u^{n-1})^2+\mathcal{E}_u^n\mathcal{E}_u^{n-1}\right)\end{aligned}$$

$$
\begin{aligned}
&+ C_0^2 \frac{\tau_n^2 \tau_{n-1}\left(\mathcal{E}_u^n + \mathcal{E}_u^{n-1}\right) + \tau_n^3\left(\mathcal{E}_{u-1}^n + \mathcal{E}_u^{n-2}\right)}{6\tau_{n-1}(\tau_n + \tau_{n-1})}\left(\mathcal{E}_u^n + \mathcal{E}_u^{n-1}\right) \\
&+ C_0^2 \tau_n^3 \frac{\left(\tau_{n-1}\left(\mathcal{E}_u^n + \mathcal{E}_u^{n-1}\right) + \tau_n\left(\mathcal{E}_{u-1}^n + \mathcal{E}_u^{n-2}\right)\right)^2}{30\tau_{n-1}^2(\tau_n + \tau_{n-1})^2} \\
:= {} & \widetilde{\mathcal{E}}_u^{n\,2},
\end{aligned} \tag{A.24}
$$

then taking (A.24) into (A.23), we get

$$
\mathcal{B}_5 \le \sum_{n=1}^{N} 2\varepsilon^{-2} \widetilde{\mathcal{E}}_u^{n\,2} + \sum_{n=1}^{N} \int_{t_{n-1}}^{t_n} \frac{\varepsilon^4}{8} \|\nabla e_u\|^2 \, dt. \tag{A.25}
$$

Similarly, the spatial discretization error term $\mathcal{B}_9$ is estimated as follows

$$
\begin{aligned}
\mathcal{B}_9 &= \int_0^T \frac{1}{\varepsilon}\left(u_h^n - p^n, e_u\right) dt \\
&= \sum_{n=1}^{N} \frac{1}{\varepsilon} \int_{t_{n-1}}^{t_n} \left(u_h^n - R u_h^n, e_u\right) dt \\
&\le \sum_{n=1}^{N} \frac{1}{\varepsilon} \int_{t_{n-1}}^{t_n} \left\|u_h^n - R u_h^n\right\| \cdot \|e_u\| \, dt \\
&\le \sum_{n=1}^{N} \frac{1}{\varepsilon} \int_{t_{n-1}}^{t_n} \kappa(h) \left\|u_h^n - R u_h^n\right\|_{1,\Omega} \|e_u\| \, dt,
\end{aligned} \tag{A.26}
$$

where we have used Lemma A.3 in the last inequality. Since h could be small enough, the term B_9 can be ignored. With a similar argument, the term $\mathcal{B}_{13}$ can be also ignored.

Step 5: The time discretization term $\mathcal{B}_7$ is bounded as follows

$$
\begin{aligned}
\mathcal{B}_7 &= \int_0^T \left(w_h^n - w_h, -\Delta^{-1} e_u\right) dt \\
&= \sum_{n=1}^{N} \int_{t_{n-1}}^{t_n} \left((w_h^n - w_h^{n-1})\frac{t_n - t}{\tau_n} - \frac{1}{2}(t - t_{n-1})(t - t_n)\partial_n^2 w_h, -\Delta^{-1} e_u\right) dt \\
&\le \sum_{n=1}^{N} \int_{t_{n-1}}^{t_n} \left(\left\|w_h^n - w_h^{n-1}\right\|_{-1} + \left\|\frac{\tau_n^2}{8}\partial_n^2 w_h\right\|_{-1}\right) \left\|\nabla \Delta^{-1} e_u\right\| dt \\
&:= \sum_{n=1}^{N} \int_{t_{n-1}}^{t_n} \delta_w^n \cdot \left\|\nabla \Delta^{-1} e_u\right\| dt.
\end{aligned} \tag{A.27}
$$

Similarly, the terms $\mathcal{B}_8$, $\mathcal{B}_{10}$, $\mathcal{B}_{11}$, $\mathcal{B}_{14}$ are also the time discretization terms, and they are estimated as follows

$$
\begin{aligned}
\mathcal{B}_8 &= \int_0^T \varepsilon \left(\frac{A u_h^n - A u_h^{n-1}}{2}, e_u\right) dt \\
&\le \sum_{n=1}^{N} \int_{t_{n-1}}^{t_n} \varepsilon \left\|\frac{A u_h^n - A u_h^{n-1}}{2}\right\| \cdot \|e_u\| \, dt
\end{aligned}
$$

$$
:= \sum_{n=1}^{N} \int_{t_{n-1}}^{t_n} \gamma_u^n \, \|e_u\| \, dt, \tag{A.28}
$$

$$
\begin{aligned}
\mathcal{B}_{10} &= \int_0^T \left(\frac{Pf(u_h^n) - Pf(u_h^{n-1})}{2\varepsilon}, e_u \right) dt \\
&\leq \sum_{n=1}^{N} \int_{t_{n-1}}^{t_n} \left\| \frac{Pf(u_h^n) - Pf(u_h^{n-1})}{2\varepsilon} \right\| \|e_u\| \, dt \\
&:= \sum_{n=1}^{N} \int_{t_{n-1}}^{t_n} \xi_u^n \cdot \|e_u\| \, dt, \qquad \text{(A.29)} \\
\mathcal{B}_{11} &= -\int_0^T \left(\frac{w_h^n - w_h^{n-1}}{2}, e_u \right) dt \\
&\leq \sum_{n=1}^{N} \int_{t_{n-1}}^{t_n} \left\| \frac{w_h^n - w_h^{n-1}}{2} \right\| \|e_u\| \, dt \\
&:= \sum_{n=1}^{N} \int_{t_{n-1}}^{t_n} \beta_w^n \cdot \|e_u\| \, dt, \qquad \text{(A.30)} \\
\mathcal{B}_{14} &= \int_0^T \left(\frac{1}{\varepsilon} \left(u_h^n - u_h^{n-1} \right) \frac{t_n - t}{\tau_n}, e_u \right) \\
&\leq \sum_{n=1}^{N} \int_{t_{n-1}}^{t_n} \left\| \frac{u_h^n - u_h^{n-1}}{\varepsilon} \right\| \|e_u\| \, dt \\
&:= \sum_{n=1}^{N} \int_{t_{n-1}}^{t_n} \delta_u^n \cdot \|e_u\| \, dt. \qquad \text{(A.31)}
\end{aligned}
$$

Step 6: The term $\mathcal{B}_{12}$, which also contains a time discretization term, is estimated by using the definitions of w^n, w and R^n.

$$
\begin{aligned}
\mathcal{B}_{12} &= \int_0^T \Bigg(\Big(\varepsilon \mathcal{A} \Big(p(t) - p^n \Big) - \frac{1}{\varepsilon} \Big(h(p^n) \frac{t_n - t}{\tau_n} - h(p^{n-1}) \frac{t_n - t}{\tau_n} \\
&\quad - \frac{1}{2}(t - t_{n-1})(t - t_n) \frac{\frac{h(p^n) - h(p^{n-1})}{\tau_n} - \frac{h(p^{n-1}) - h(p^{n-2})}{\tau_{n-1}}}{\frac{\tau_n + \tau_{n-1}}{2}} \Big) - \Big(q(t) - q^n \Big) \Big), e_u \Bigg) dt \\
&= \sum_{n=1}^{N} \int_{t_{n-1}}^{t_n} \Bigg(\Big(\varepsilon \mathcal{A} \Big(p^n \frac{t - t_{n-1}}{\tau_n} + p^{n-1} \frac{t_n - t}{\tau_n} + \frac{1}{2}(t - t_{n-1})(t - t_n) \partial_n^2 p - p^n \Big) \\
&\quad - \frac{1}{\varepsilon} \Big(h(p^n) - h(p^{n-1}) \Big) \frac{t_n - t}{\tau_n} + \frac{1}{2\varepsilon}(t - t_{n-1})(t - t_n) \frac{\frac{h(p^n) - h(p^{n-1})}{\tau_n} - \frac{h(p^{n-1}) - h(p^{n-2})}{\tau_{n-1}}}{\frac{\tau_n + \tau_{n-1}}{2}} \\
&\quad - \Big(q^n \frac{t - t_{n-1}}{\tau_n} + q^{n-1} \frac{t_n - t}{\tau_n} + \frac{1}{2}(t - t_{n-1})(t - t_n) \partial_n^2 q - q^n \Big) \Big), e_u \Bigg) dt \\
&= \sum_{n=1}^{N} \int_{t_{n-1}}^{t_n} \Bigg(\Big(\Big(\varepsilon \mathcal{A} R u_h^{n-1} + \frac{1}{\varepsilon} h(R u_h^{n-1}) - q^{n-1} \Big) - \Big(\varepsilon \mathcal{A} R u_h^n + \frac{1}{\varepsilon} h(R u_h^n) - q^n \Big) \Big) \frac{t_n - t}{\tau_n}
\end{aligned}
$$

$$
+\frac{\frac{(\varepsilon\mathcal{A}p^n+\frac{h(p^n)}{\varepsilon}-q^n)-(\varepsilon\mathcal{A}p^{n-1}+\frac{h(p^{n-1})}{\varepsilon}-q^{n-1})}{\tau_n}-\frac{(\varepsilon\mathcal{A}p^{n-1}+\frac{h(p^{n-1})}{\varepsilon}-q^{n-1})-(\varepsilon\mathcal{A}p^{n-2}+\frac{h(p^{n-2})}{\varepsilon}-q^{n-2})}{\tau_{n-1}}}{\frac{\tau_n+\tau_{n-1}}{2}}
$$

$$
\frac{(t-t_{n-1})(t-t_n)}{2}, e_u\Big)dt
$$

$$
\leq \sum_{n=1}^{N}\int_{t_{n-1}}^{t_n}\Big(2\Big\|\Big(\varepsilon A u_h^{n-1}+\frac{1}{\varepsilon}h(u_h^{n-1})-w_h^{n-1}\Big)-\Big(\varepsilon A u_h^{n}+\frac{1}{\varepsilon}h(u_h^{n})-w_h^{n}\Big)\Big\|
$$

$$
+\Big\|\Big(\varepsilon A u_h^{n-1}+\frac{1}{\varepsilon}h(u_h^{n-1})-w_h^{n-1}\Big)-\Big(\varepsilon A u_h^{n-2}+\frac{1}{\varepsilon}h(u_h^{n-2})-w_h^{n-2}\Big)\Big\|\Big)\cdot\|e_u\|dt
$$

$$
=\sum_{n=1}^{N}\int_{t_{n-1}}^{t_n}\theta_u^n\cdot\|e_u\|dt. \tag{A.32}
$$

Step 7: The term $\mathcal{B}_{15}$ also yields a time discretization error, which is estimated by using Lagrange mean value theorem and embedding theorem.

$$
\mathcal{B}_{15}=\int_0^T\Big(\frac{1}{\varepsilon}\Big(f(u_h^n)\frac{t-t_{n-1}}{\tau_n}+f(u_h^{n-1})\frac{t_n-t}{\tau_n}-f(p^n)+f(p^n)\frac{t_n-t}{\tau_n}-f(p^{n-1})\frac{t_n-t}{\tau_n}\Big)
$$

$$
+\frac{1}{2\varepsilon}(t-t_{n-1})(t-t_n)
$$

$$
\left(\frac{\frac{f(u_h^n)-f(u_h^{n-1})}{\tau_n}-\frac{f(u_h^{n-1})-f(u_h^{n-2})}{\tau_{n-1}}}{\frac{\tau_n+\tau_{n-1}}{2}}-\frac{\frac{f(p^n)-f(p^{n-1})}{\tau_n}-\frac{f(p^{n-1})-f(p^{n-2})}{\tau_{n-1}}}{\frac{\tau_n+\tau_{n-1}}{2}}\right), e_u\Big)dt
$$

$$
\leq\sum_{n=1}^{N}\int_{t_{n-1}}^{t_n}\left(\frac{t-t_{n-1}}{\tau_n\varepsilon}\left(f(u_h^n)-f(p^n)\right), e_u\right)dt
$$

$$
+\sum_{n=1}^{N}\int_{t_{n-1}}^{t_n}\left(\frac{t_n-t}{\tau_n\varepsilon}\left(f(u_h^{n-1})-f(p^{n-1})\right), e_u\right)dt
$$

$$
+\sum_{n=1}^{N}\int_{t_{n-1}}^{t_n}\left(\frac{1}{2\varepsilon}(t-t_{n-1})(t-t_n)\frac{\frac{f(u_h^n)-f(p^n)}{\tau_n}}{\frac{\tau_n+\tau_{n-1}}{2}}, e_u\right)dt
$$

$$
+\sum_{n=1}^{N}\int_{t_{n-1}}^{t_n}\left(\frac{1}{\varepsilon}(t-t_{n-1})(t-t_n)\frac{\frac{f(u_h^{n-1})-f(p^{n-1})}{\tau_n}}{\frac{\tau_n+\tau_{n-1}}{2}}, e_u\right)dt
$$

$$
+\sum_{n=1}^{N}\int_{t_{n-1}}^{t_n}\left(\frac{1}{2\varepsilon}(t-t_{n-1})(t-t_n)\frac{\frac{f(u_h^{n-2})-f(p^{n-2})}{\tau_n}}{\frac{\tau_n+\tau_{n-1}}{2}}, e_u\right)dt
$$

$$
\leq\sum_{n=1}^{N}\int_{t_{n-1}}^{t_n}\frac{3}{2\varepsilon}\left\|f'(\xi_1)\right\|_{0,3,\Omega}\cdot\left\|u_h^n-p^n\right\|_{0,6,\Omega}\cdot\|e_u\|\,dt
$$

$$
+\sum_{n=1}^{N}\int_{t_{n-1}}^{t_n}\frac{2}{\varepsilon}\left\|f'(\xi_2)\right\|_{0,3,\Omega}\cdot\left\|u_h^{n-1}-p^{n-1}\right\|_{0,6,\Omega}\cdot\|e_u\|\,dt
$$

$$
+\sum_{n=1}^{N}\int_{t_{n-1}}^{t_n}\frac{1}{2\varepsilon}\left\|f'(\xi_3)\right\|_{0,3,\Omega}\cdot\left\|u_h^{n-2}-p^{n-2}\right\|_{0,6,\Omega}\cdot\|e_u\|\,dt
$$

$$
\begin{aligned}
&\le \sum_{n=1}^{N} \int_{t_{n-1}}^{t_n} \frac{3}{2\varepsilon} \left\| f'(\xi_1) \right\|_{1,\Omega} \cdot \left\| u_h^n - p^n \right\|_{1,\Omega} \cdot \| e_u \| \, dt \\
&\quad + \sum_{n=1}^{N} \int_{t_{n-1}}^{t_n} \frac{2}{\varepsilon} \left\| f'(\xi_2) \right\|_{1,\Omega} \cdot \left\| u_h^{n-1} - p^{n-1} \right\|_{1,\Omega} \cdot \| e_u \| \, dt \\
&\quad + \sum_{n=1}^{N} \int_{t_{n-1}}^{t_n} \frac{1}{2\varepsilon} \left\| f'(\xi_3) \right\|_{1,3,\Omega} \cdot \left\| u_h^{n-2} - p^{n-2} \right\|_{1,6,\Omega} \cdot \| e_u \| \, dt \\
&\le \sum_{n=1}^{N} \int_{t_{n-1}}^{t_n} \frac{1}{\varepsilon} C \mathcal{E}_u^n \| e_u \| \, dt + \sum_{n=1}^{N} \int_{t_{n-1}}^{t_n} \frac{1}{\varepsilon} C \mathcal{E}_u^{n-1} \| e_u \| \, dt + \sum_{n=1}^{N} \int_{t_{n-1}}^{t_n} \frac{1}{\varepsilon} C \mathcal{E}_u^{n-2} \| e_u \| \, dt \\
&:= \sum_{n=1}^{N} \int_{t_{n-1}}^{t_n} \alpha_u^n \| e_u \| \, dt. \qquad \text{(A.33)}
\end{aligned}
$$

Step 8: In order to estimate the term $\mathcal{B}_{16}$, which also yields a time discretization error, we first simplify the following formula

$$
\begin{aligned}
&f(u_h) - f(u_h^n) \frac{t - t_{n-1}}{\tau_n} - f(u_h^{n-1}) \frac{t_n - t}{\tau_n} - \frac{1}{2}(t - t_{n-1})(t - t_n) \\
&\frac{\frac{f(u_h^n) - f(u_h^{n-1})}{\tau_n} - \frac{f(u_h^{n-1}) - f(u_h^{n-2})}{\tau_{n-1}}}{\frac{\tau_n + \tau_{n-1}}{2}} \\
&\quad = \left[3(u_h^n)^2 u_h^{n-1} - 2(u_h^n)^3 - (u_h^{n-1})^3 \right] \cdot \left(\frac{t - t_{n-1}}{\tau_n} \right)^2 \frac{t_n - t}{\tau_n} \\
&\quad + \left[3u_h^n (u_h^{n-1})^2 - (u_h^n)^3 - 2(u_h^{n-1})^3 \right] \cdot \frac{t - t_{n-1}}{\tau_n} \left(\frac{t_n - t}{\tau_n} \right)^2 \\
&\quad + \left[3(u_h^n)^2 \partial_n^2 u_h - 3u_h^n u_h^{n-1} \partial_n^2 u_h \right] \cdot \frac{1}{2}(t - t_{n-1})(t - t_n) \left(\frac{t - t_{n-1}}{\tau_n} \right)^2 \\
&\quad + \left[3(u_h^{n-1})^2 \partial_n^2 u_h - 3u_h^n u_h^{n-1} \partial_n^2 u_h \right] \cdot \frac{1}{2}(t - t_{n-1})(t - t_n) \left(\frac{t_n - t}{\tau_n} \right)^2 \\
&\quad + \left[3u_h^n u_h^{n-1} \partial_n^2 u_h - \frac{\frac{(u_h^n)^3 - (u_h^{n-1})^3}{\tau_n} - \frac{(u_h^{n-1})^3 - (u_h^{n-2})^3}{\tau_{n-1}}}{\frac{\tau_n + \tau_{n-1}}{2}} \right] \cdot \frac{1}{2}(t - t_{n-1})(t - t_n) \\
&\quad + \left[\left(3u_h^n (\partial_n^2 u_h)^2 - 3u_h^{n-1} (\partial_n^2 u_h)^2 \right) \cdot \left(\frac{t - t_{n-1}}{\tau_n} \right) + 3u_h^{n-1} (\partial_n^2 u_h)^2 \right] \\
&\quad \cdot \left(\frac{1}{2}(t - t_{n-1})(t - t_n) \right)^2 + \left[\left(\frac{1}{2}(t - t_{n-1})(t - t_n) \right)^3 (\partial_n^2 u_h)^3 \right], \qquad \text{(A.34)}
\end{aligned}
$$

thus we have

$$
\begin{aligned}
\mathcal{B}_{16} = \int_0^T \Bigg(\frac{1}{\varepsilon} \Bigg(& f(u_h) - f(u_h^n) \frac{t - t_{n-1}}{\tau_n} - f(u_h^{n-1}) \frac{t_n - t}{\tau_n} \\
& - \frac{1}{2}(t - t_{n-1})(t - t_n) \frac{\frac{f(u_h^n) - f(u_h^{n-1})}{\tau_n} - \frac{f(u_h^{n-1}) - f(u_h^{n-2})}{\tau_{n-1}}}{\frac{\tau_n + \tau_{n-1}}{2}} \Bigg), e_u \Bigg) dt
\end{aligned}
$$

$$
\begin{aligned}
&= \sum_{n=1}^{N} \int_{t_{n-1}}^{t_n} \frac{1}{\varepsilon} \Big(\Big[3(u_h^n)^2 u_h^{n-1} - 2(u_h^n)^3 - (u_h^{n-1})^3 \Big] \cdot \Big(\frac{t - t_{n-1}}{\tau_n} \Big)^2 \frac{t_n - t}{\tau_n} \\
&+ \Big[3u_h^n (u_h^{n-1})^2 - (u_h^n)^3 - 2(u_h^{n-1})^3 \Big] \cdot \frac{t - t_{n-1}}{\tau_n} \Big(\frac{t_n - t}{\tau_n} \Big)^2 \\
&+ \Big[3(u_h^n)^2 \partial_n^2 u_h - 3u_h^n u_h^{n-1} \partial_n^2 u_h \Big] \cdot \frac{1}{2}(t - t_{n-1})(t - t_n) \left(\frac{t - t_{n-1}}{\tau_n} \right)^2 \\
&+ \Big[3(u_h^{n-1})^2 \partial_n^2 u_h - 3u_h^n u_h^{n-1} \partial_n^2 u_h \Big] \cdot \frac{1}{2}(t - t_{n-1})(t - t_n) \left(\frac{t_n - t}{\tau_n} \right)^2 \\
&+ \Bigg[3u_h^n u_h^{n-1} \partial_n^2 u_h - - \frac{\frac{(u_h^n)^3 - (u_h^{n-1})^3}{\tau_n} - \frac{(u_h^{n-1})^3 - (u_h^{n-2})^3}{\tau_{n-1}}}{\frac{\tau_n + \tau_{n-1}}{2}} \Bigg] \cdot \frac{1}{2}(t - t_{n-1})(t - t_n) \\
&+ \Big[\Big(3u_h^n (\partial_n^2 u_h)^2 - 3u_h^{n-1} (\partial_n^2 u_h)^2 \Big) \cdot \left(\frac{t - t_{n-1}}{\tau_n} \right) + 3u_h^{n-1} (\partial_n^2 u_h)^2 \Big] \cdot \Big(\frac{1}{2}(t - t_{n-1})(t - t_n) \Big)^2 \\
&+ \Big[\Big(\frac{1}{2}(t - t_{n-1})(t - t_n) \Big)^3 (\partial_n^2 u_h)^3 \Big], e_u \Big) dt \\
&\le \sum_{n=1}^{N} \int_{t_{n-1}}^{t_n} \left\| \frac{3(u_h^n)^2 u_h^{n-1} - 2(u_h^n)^3 - (u_h^{n-1})^3}{\varepsilon} \right\| \cdot \|e_u\| \, dt \\
&+ \sum_{n=1}^{N} \int_{t_{n-1}}^{t_n} \left\| \frac{3u_h^n (u_h^{n-1})^2 - 2(u_h^{n-1})^3 - (u_h^n)^3}{\varepsilon} \right\| \cdot \|e_u\| \, dt \\
&+ \sum_{n=1}^{N} \int_{t_{n-1}}^{t_n} \left\| \frac{\big(3(u_h^n)^2 \partial_n^2 u_h - 3u_h^n u_h^{n-1} \partial_n^2 u_h \big) \tau_n^2}{8\varepsilon} \right\| \cdot \|e_u\| \, dt \\
&+ \sum_{n=1}^{N} \int_{t_{n-1}}^{t_n} \left\| \frac{\big(3(u_h^{n-1})^2 \partial_n^2 u_h - 3u_h^n u_h^{n-1} \partial_n^2 u_h \big) \tau_n^2}{8\varepsilon} \right\| \cdot \|e_u\| \, dt \\
&+ \sum_{n=1}^{N} \int_{t_{n-1}}^{t_n} \left\| \frac{\Big(3u_h^n u_h^{n-1} \partial_n^2 u_h - \frac{\frac{(u_h^n)^3 - (u_h^{n-1})^3}{\tau_n} - \frac{(u_h^{n-1})^3 - (u_h^{n-2})^3}{\tau_{n-1}}}{\frac{\tau_n + \tau_{n-1}}{2}} \Big) \tau_n^2}{8\varepsilon} \right\| \cdot \|e_u\| \, dt \\
&+ \sum_{n=1}^{N} \int_{t_{n-1}}^{t_n} \left(\left\| \frac{\big(3u_h^n (\partial_n^2 u_h)^2 - 3u_h^{n-1} (\partial_n^2 u_h)^2 \big) \tau_n^4}{64\varepsilon} \right\| + \left\| \frac{\big(3u_h^{n-1} (\partial_n^2 u_h)^2 \big) \tau_n^4}{64\varepsilon} \right\| \right) \cdot \|e_u\| \, dt \\
&+ \sum_{n=1}^{N} \int_{t_{n-1}}^{t_n} \left(\left\| \frac{(\partial_n^2 u_h)^3 \tau_n^6}{512\varepsilon} \right\| \right) \cdot \|e_u\| \, dt \\
&:= \sum_{n=1}^{N} \int_{t_{n-1}}^{t_n} \zeta_u^n \, \|e_u\| \, dt.
\end{aligned} \tag{A.35}
$$

Step 9: Grouping together (A.19)–(A.22), (A.26) and (A.27), we have

$$
\begin{aligned}
&\mathcal{B}_1 + \cdots + \mathcal{B}_4 + \mathcal{B}_6 + \mathcal{B}_7 \\
&\qquad \le \sum_{n=1}^{N} \int_{t_{n-1}}^{t_n} \gamma_w^n \left\| \nabla \Delta^{-1} e_u \right\| dt + \sum_{n=1}^{N} \int_{t_{n-1}}^{t_n} \beta_u^n \left\| \nabla \Delta^{-1} e_u \right\| dt
\end{aligned}
$$

$$
\begin{aligned}
&+\sum_{n=1}^{N}\int_{t_{n-1}}^{t_n}\delta_w^n\cdot\left\|\nabla\Delta^{-1}e_u\right\|dt+\sum_{n=1}^{N}\int_{t_{n-1}}^{t_n}\eta_w^n\cdot\left\|\nabla\Delta^{-1}e_u\right\|dt\\
:=&\sum_{n=1}^{N}\int_{t_{n-1}}^{t_n}\eta_0\left\|\nabla\Delta^{-1}e_u\right\|dt\\
\le&\sum_{n=1}^{N}\int_{t_{n-1}}^{t_n}\frac{1}{2}\eta_0^2dt+\sum_{n=1}^{N}\int_{t_{n-1}}^{t_n}\frac{1}{2}\left\|\nabla\Delta^{-1}e_u\right\|^2dt. \qquad (A.36)
\end{aligned}
$$

Summing up (A.28)–(A.33) and (A.35), it holds that

$$
\begin{aligned}
\mathcal{B}_8+\cdots+\mathcal{B}_{16}\le&\sum_{n=1}^{N}\int_{t_{n-1}}^{t_n}\gamma_u^n\|e_u\|\,dt+\sum_{n=1}^{N}\int_{t_{n-1}}^{t_n}\xi_u^n\|e_u\|\,dt+\sum_{n=1}^{N}\int_{t_{n-1}}^{t_n}\beta_w^n\|e_u\|\,dt\\
&+\sum_{n=1}^{N}\int_{t_{n-1}}^{t_n}\theta_u^n\cdot\|e_u\|dt+\sum_{n=1}^{N}\int_{t_{n-1}}^{t_n}\delta_u^n\cdot\|e_u\|\,dt\\
&+\sum_{n=1}^{N}\int_{t_{n-1}}^{t_n}\alpha_u^n\|e_u\|\,dt+\sum_{n=1}^{N}\int_{t_{n-1}}^{t_n}\zeta_u^n\|e_u\|\,dt\\
:=&\sum_{n=1}^{N}\int_{t_{n-1}}^{t_n}\eta_1\|e_u\|\,dt\\
\le&\sum_{n=1}^{N}\int_{t_{n-1}}^{t_n}\frac{1}{2\varepsilon^2}\eta_1^2dt+\sum_{n=1}^{N}\int_{t_{n-1}}^{t_n}\frac{\varepsilon^2}{2}\|e_u\|^2dt. \qquad (A.37)
\end{aligned}
$$

Step 10: Notice that [4]

$$
f(a_1)-f(a_2)-f'(a_2)(a_1-a_2)=3a_2(a_1-a_2)^2+(a_1-a_2)^3,
$$

then

$$
\begin{aligned}
\left(f(a_1)-f(a_2)-f'(a_2)(a_1-a_2)\right)(a_1-a_2)&=3a_2(a_1-a_2)^3+(a_1-a_2)^4\\
&\ge-\tilde f(a_2)\mid a_1-a_2\mid^3 \qquad (A.38)
\end{aligned}
$$

with $\tilde f(a_2)=3|a_2|$. Therefore, according to (A.38) and the spectrum estimate [1, 9], we obtain the following estimation for the term $\mathcal{B}_{17}$

$$
\begin{aligned}
\mathcal{B}_{17}=&\int_0^T\left(\frac{1}{\varepsilon}\left(f(u)-f(u_h)\right),e_u\right)dt\\
\le&\int_0^T\left(-\frac{1}{\varepsilon}\left(f'(u_h)e_u,e_u\right)+\frac{1}{\varepsilon}\left(\tilde f(u_h),|u-u_h|^3\right)\right)dt\\
\le&\int_0^T\left(-\frac{1-\varepsilon^3}{\varepsilon}\left(f'(u_h)e_u,e_u\right)-\varepsilon^2\left(f'(u_h)e_u,e_u\right)+\frac{1}{\varepsilon}\left(\tilde f(u_h),|u-u_h|^3\right)\right)dt\\
\le&\int_0^T\left(\left(1-\varepsilon^3\right)\overline{\Lambda}_h(t)\|\nabla\Delta^{-1}e_u\|^2+\varepsilon\left(1-\varepsilon^3\right)\|\nabla e_u\|^2+2\varepsilon^2\|e_u\|^2+\frac{1}{\varepsilon}\mu_g\|e_u\|_{L^3}^3\right)dt, \qquad (A.39)
\end{aligned}
$$

here $\mu_g:=\sup_{t\in(0,T)}\|\tilde f(u_h)\|_{L^\infty(\Omega)}$.

Step 11: Taking (A.25), (A.36) and (A.39) into (A.18), we have

$$\begin{aligned}\frac{1}{2}\|\nabla\Delta^{-1}e_u^N\|^2+\int_0^T \varepsilon\|\nabla e_u\|^2dt\leq&\frac{1}{2}\|\nabla\Delta^{-1}e_u^0\|^2+\sum_{n=1}^N 2\varepsilon^{-2}\widetilde{\mathcal{E}}_u^{n2}+\sum_{n=1}^N\int_{t_{n-1}}^{t_n}\frac{\varepsilon^4}{8}\|\nabla e_u\|^2\,dt\\&+\sum_{n=1}^N\int_{t_{n-1}}^{t_n}\frac{1}{2}\eta_0^2dt+\sum_{n=1}^N\int_{t_{n-1}}^{t_n}\frac{1}{2}\left\|\nabla\Delta^{-1}e_u\right\|^2dt\\&+\sum_{n=1}^N\int_{t_{n-1}}^{t_n}\frac{1}{2\varepsilon^2}\eta_1^2dt+\sum_{n=1}^N\int_{t_{n-1}}^{t_n}\frac{\varepsilon^2}{2}\|e_u\|^2\,dt\\&+\int_0^T\left(1-\varepsilon^3\right)\overline{\Lambda}_h(t)\|\nabla\Delta^{-1}e_u\|^2dt\\&+\sum_{n=1}^N\int_{t_{n-1}}^{t_n}2\varepsilon^2\|e_u\|^2\,dt+\int_0^T\varepsilon\left(1-\varepsilon^3\right)\|\nabla e_u\|^2dt\\&+\int_0^T\frac{1}{\varepsilon}\mu_g\|e_u\|_{L^3}^3dt.\end{aligned}\tag{A.40}$$

Note that

$$\begin{aligned}\frac{5\varepsilon^2}{2}\|e_u\|^2&=\frac{5\varepsilon^2}{2}\left(\nabla(-\Delta^{-1}e_u),\nabla e_u\right)\\&\leq\sqrt{5}\|\nabla\Delta^{-1}e_u\|\cdot\frac{\sqrt{5}\varepsilon^2}{2}\|\nabla e_u\|\\&\leq\frac{5}{2}\|\nabla\Delta^{-1}e_u\|^2+\frac{5\varepsilon^4 8}{\|}\nabla e_u\|^2,\end{aligned}\tag{A.41}$$

plugging (A.41) into (A.40), and further simplification, then we obtain

$$\begin{aligned}&\|\nabla\Delta^{-1}e_u^N\|^2+\int_0^T\frac{\varepsilon^4}{2}\|\nabla e_u\|^2dt\\&\leq\|\nabla\Delta^{-1}e_u^0\|^2+\sum_{n=1}^N 4\varepsilon^{-2}\widetilde{\mathcal{E}}_u^{n2}+\sum_{n=1}^N\left(\eta_0^2+\varepsilon^{-2}\eta_1^2\right)\tau_n\\&+\int_0^T\left(6+2\left(1-\varepsilon^3\right)\overline{\Lambda}_h(t)\right)\|\nabla\Delta^{-1}e_u\|^2dt\\&+\int_0^T\frac{2}{\varepsilon}\mu_g\|e_u\|_{L^3}^3dt.\end{aligned}\tag{A.42}$$

Let

$$y_1(t):=\|\nabla\Delta^{-1}e_u\|^2,\qquad y_2(t):=\frac{\varepsilon^4}{2}\|\nabla e_u\|^2,\qquad y_3(t):=2\varepsilon^{-1}\mu_g\|e_u\|_{L^3}^3,$$

$$\eta^2:=\|\nabla\Delta^{-1}e_u^0\|^2+\sum_{n=1}^N 4\varepsilon^{-2}\widetilde{\mathcal{E}}_u^{n2}+\sum_{n=1}^N\left(\eta_0^2+\varepsilon^{-2}\eta_1^2\right)\tau_n.$$

According to Lemma A.1 and assume that $\|e_u\|_{L^\infty}\leq C$, it holds that

$$\int_0^T 2\varepsilon^{-1}\mu_g\|e_u\|_{L^3}^3dt\leq\int_0^T 2\varepsilon^{-1}\mu_g C_I\|e_u\|_{L^\infty(\Omega)}^{1-\sigma}\|\nabla\Delta^{-1}e_u\|^\sigma\|\nabla e_u\|^2dt$$

$$\leq \int_0^T 2\varepsilon^{-1}\mu_g C_I \|e_u\|_{L^\infty(\Omega)}^{1-\sigma} \|\nabla\Delta^{-1}e_u\|^\sigma \|\nabla e_u\|^2 dt$$
$$\leq 2\varepsilon^{-1}\mu_g C_S \left(\sup_{t\in(0,T)} \|\nabla\Delta^{-1}e_u\|^\sigma \right) \int_0^T \|\nabla e_u\|^2 dt$$
$$\leq B \left(\sup_{t\in(0,T)} \|\nabla\Delta^{-1}e_u\|^\sigma \right) \int_0^T \left(\|\nabla e_u\|^2 + \|\nabla\Delta^{-1}e_u\|^2 \right) dt,$$

with $B := 2\varepsilon^{-1}\mu_g C_S$. Setting

$$E := \exp\left(\int_0^T a(t)dt \right), \qquad \beta := \sigma, \qquad A = \eta^2,$$

and based on the assumption on A shown in Lemma A.2, we have

$$\eta^2 \leq \frac{\varepsilon^{1/\sigma}}{(2\mu_g C_S(1+T))^{1/\sigma}} \left(8\exp\left(\int_0^T a(t)dt \right) \right)^{-1-\frac{1}{\sigma}}.$$

Therefore, by using Lemma A.2, we obtain

$$\sup_{t\in[0,T]} \|\nabla\Delta^{-1}e_u\|^2 + \int_0^T \frac{\varepsilon^4}{2} \|\nabla e_u\|^2 dt \leq 8\eta^2 \exp\left(\int_0^T a(t)dt \right).$$

□

References

1. Alikakos, N.D., Fusco, G.: The spectrum of the Cahn–Hilliard operator for generic interface in higher space dimensions. Indiana Univ. Math. J. **42**(2), 637–674 (1993)
2. Bartels, S.: A posteriori error analysis for time-dependent Ginzburg–Landau type equations. Numer. Math. **99**, 557–583 (2005)
3. Bartels, S., Müller, R.: Error control for the approximation of Allen–Cahn and Cahn–Hilliard equations with a logarithmic potential. Numer. Math. **119**(3), 409–435 (2011)
4. Bartels, S., Müller, R.: Quasi-optimal and robust a posteriori error estimates in $L^\infty(L^2)$ for the approximation of Allen–Cahn equations past singularities. Math. Comput. **80**(274), 761–780 (2011)
5. Bartels, S., Müller, R., Ortner, C.: Robust a priori and a posteriori error analysis for the approximation of Allen–Cahn and Ginzburg–Landau equations past topological changes. SIAM J. Numer. Anal. **49**, 110–134 (2011)
6. Bates, P.W., Fife, P.C.: The dynamics of nucleation for the Cahn–Hilliard equation. SIAM J. Appl. Math. **53**(4), 990–1008 (1993)
7. Bramble, J.H., Schatz, A.H.: Higher order local accuracy by averaging in the finite element method. Math. Comput. **31**, 74–111 (1977)
8. Cahn, J.W., Hilliard, J.E.: Free energy of a nonuniform system. I. Interfacial free energy. J. Chem. Phys. **28**(2), 258–267 (1958)
9. Chen, X.: Spectrum for the Allen–Cahn, Cahn–Hilliard, and phase-field equations for generic interfaces. Commun. Part. Differ. Equ. **19**(7–8), 1371–1395 (1994)
10. Chen, Y., Huang, Y., Yi, N.: A SCR-based error estimation and adaptive finite element method for the Allen–Cahn equation. Comput. Math. Appl. **78**, 204–223 (2019)
11. Chen, Y., Huang, Y., Yi, N.: Recovery type a posteriori error estimation of adaptive finite element method for Allen–Cahn equation. J. Comput. Appl. Math. **369**, 112574 (2019)
12. Cheng, K., Feng, W., Wang, C., Wise, S.: An energy stable fourth order finite difference scheme for the Cahn–Hilliard equation. J. Comput. Appl. Math. **362**, 574–595 (2019)
13. Chrysafinos, K., Georgoulis, E., Plaka, D.: A posteriori error estimates for the Allen–Cahn problem. SIAM J. Numer. Anal. **58**(5), 2662–2683 (2020)

14. Diegel, A., Cheng, C., Wise, S.: Stability and convergence of a second-order mixed finite element method for the Cahn–Hilliard equation. IMA J. Numer. Anal. **36**(4), 1867–1897 (2016)
15. Du, Q., Nicolaides, R.: Numerical analysis of a continuum model of phase transition. SIAM J. Numer. Anal. **28**(5), 1310–1322 (1991)
16. Elliott, C.M., French, D.A.: Numerical studies of the Cahn–Hilliard equation for phase separation. IMA J. Appl. Math. **38**(2), 97–128 (1987)
17. Elliott, C.M., Songmu, Z.: On the Cahn–Hilliard equation. Arch. Rational Mech. Anal. **96**, 339–357 (1986)
18. Feng, X., Karakashian, O.A.: Fully discrete dynamic mesh discontinuous Galerkin methods for the Cahn–Hilliard equation of phase transition. Math. Comput. **76**, 1093–1117 (2007)
19. Feng, X., Li, Y., Xing, Y.: Analysis of mixed interior penalty discontinuous Galerkin methods for the Cahn–Hilliard equation and the Hele–Shaw flow. SIAM J. Numer. Anal. **54**(2), 825–847 (2016)
20. Feng, X., Prohl, A.: Error analysis of a mixed finite element method for the Cahn–Hilliard equation. Numer. Math. **99**(1), 47–84 (2004)
21. Feng, X., Wu, H.: A posteriori error estimates for finite element approximations of the Cahn–Hilliard equation and the Hele–Shaw flow. J. Comput. Math. **26**(6), 767–796 (2008)
22. Georgoulis, E., Makridakis, C.: On a posteriori error control for the Allen–Cahn problem. Math. Methods Appl. Sci. **37**(2), 173–179 (2014)
23. Grisvard, P.: Elliptic Problems in Nonsmooth Domains. Pitman, Boston (1985)
24. Grisvard, P.: Singularities in Boundary Value Problems. Research Notes in Applied Mathematics. Springer, New York (1992)
25. Guo, J., Wang, C., Wise, S., Yue, X.: An H^2 convergence of a second-order convex-splitting, finite difference scheme for the three-dimensional Cahn-Hilliard equation. Commun. Math. Sci. **14**(2), 489–515 (2016)
26. He, L., Zhou, A.: Adaptive finite element analysis for semilinear elliptic problems (in Chinese). Sci. Sin. Math. **46**(7), 929–944 (2016)
27. Heimsund, B., Tai, X., Wang, J.: Superconvergence for the gradient of the finite element approximations by L^2-projections. SIAM J. Numer. Anal. **40**, 1538–1560 (2002)
28. Hou, D., Azaiez, M., Xu, C.: A variant of scalar auxiliary variable approaches for gradient flows. J. Comput. Phys. **395**, 307–332 (2019)
29. Huang, Y., Jiang, K., Yi, N.: Some weighted averaging methods for gradient recovery. Adv. Appl. Math. Mech. **4**, 131–155 (2012)
30. Huang, Y., Liu, H., Yi, N.: Recovery of interface derivatives from the piecewise L^2 projection. J. Comput. Phys. **231**, 1230–1243 (2012)
31. Huang, Y., Yi, N.: The superconvergent cluster recovery method. J. Sci. Comput. **44**, 301–322 (2010)
32. Jia, H., Li, Y., Feng, G., Li, K.: An efficient two-grid method for the Cahn–Hilliard equation with the concentration-dependent mobility and the logarithmic Flory-Huggins bulk potential. Appl. Math. Comput. **387**, 124548 (2020)
33. Lakkis, O., Makridakis, C.: Elliptic reconstruction and a posteriori error estimates for fully discrete linear parabolic problems. Math. Comput. **75**(256), 1627–1658 (2006)
34. Lakkis, O., Pryer, T.: Gradient recovery in adaptive finite-element methods for parabolic problem. IMA J. Numer. Anal. **32**(1), 246–278 (2012)
35. Li, H., Yin, P., Zhang, Z.: A C^0 finite element method for the biharmonic problem with Navier boundary conditions in a polygonal domain. IMA J. Numer. Anal. **43**, 1779–1801 (2023)
36. Lin, Q., Yan, N.: Construction and Analysis of High Efficient Finite Elements. Hebei University Press, Baoding (1996) (**in Chinese**)
37. Liu, H., Yin, P.: Unconditionally energy stable DG schemes for the Cahn–Hilliard equation. J. Comput. Appl. Math. **390**, 113375 (2021)
38. Lozinski, A., Picasso, M., Prachittham, V.: An anisotropic error estimator for the Crank–Nicolson method: application to a parabolic problem. SIAM J. Sci. Comput. **31**(4), 2757–2783 (2009)
39. Makridakis, C., Nochetto, R.H.: Elliptic reconstruction and a posteriori error estimates for parabolic problems. SIAM J. Numer. Anal. **41**(4), 1585–1594 (2004)
40. Shen, J., Xu, J., Yang, J.: The scalar auxiliary variable (SAV) approach for gradient flows. J. Comput. Phys. **353**, 407–416 (2018)
41. Shen, J., Xu, J., Yang, J.: A new class of efficient and robust energy stable schemes for gradient flows. SIAM Rev. **61**(3), 474–506 (2019)
42. Shen, J., Yang, X.: Numerical approximations of Allen–Cahn and Cahn–Hilliard equations. Discrete Contin. Dyn. Syst. Ser. A **28**, 1669–1691 (2010)
43. Wells, G., Kuhl, E., Garikipati, K.: A discontinuous Galerkin method for the Cahn–Hilliard equation. J. Comput. Phys. **218**(2), 860–877 (2006)

44. Yan, N.: Superconvergence Analysis and a Posteriori Error Estimation in Finite Element Methods. Science Press, Beijing (2008)
45. Yang, X., Zhao, J., Wang, Q., Shen, J.: Numerical approximations for a three components Cahn–Hilliard phase-field model based on the invariant energy quadratization method. Math. Models Methods Appl. Sci. **27**(11), 1–38 (2017)
46. Yi, N.: A posteriori error estimates based on gradient recovery and adaptive finite element methods. Ph.D. thesis, Xiangtan University (2011)
47. Zienkiewicz, O.C., Zhu, J.Z.: The supercovergent patch recovery and a posteriori error estimates. Int. J. Numer. Methods Eng. **33**, 331–1382 (1992)
48. Zhang, Z., Naga, A.: A new finite element gradient recovery method: superconvergence property. SIAM J. Sci. Comput. **26**, 1192–1213 (2005)